T.R.

GEBZE TECHNICAL UNIVERSITY

GRADUATE SCHOOL OF NATURAL AND APPLIED SCIENCES

MATHEMATICAL MODELING OF MEAT FREEZE-DRYING IN TRAYS AND PARAMETER ESTIMATION

ÖZNUR CUMHUR

A THESIS SUBMITTED FOR THE DEGREE OF

DOCTOR OF PHILOSOPHY

DEPARTMENT OF CHEMICAL ENGINEERING

GEBZE

2015

T.R.

GEBZE TECHNICAL UNİVERSITY

GRADUATE SCHOOL OF NATURAL AND APPLIED SCIENCES

MATHEMATICAL MODELING OF MEAT FREEZE-DRYING IN TRAYS AND PARAMETER ESTIMATION

ÖZNUR CUMHUR

A THESIS SUBMITTED FOR THE DEGREE OF DOCTOR OF PHILOSOPHY

DEPARTMENT OF CHEMICAL ENGINEERING

THESIS SUPERVISOR

ASSOC. PROF. DR. MAHMUT ŞEKER

II. THESIS SUPERVISOR

PROF. DR. HASAN SADIKOGLU

GEBZE

2015

T.C.
GEBZE TEKNİK ÜNİVERSİTESİ
FEN BİLİMLERİ ENSTİTÜSÜ

ETİN DONDURARAK KURUTMA İŞLEMİNİN MATEMATİKSEL MODELLENMESİ VE PARAMETRELERİN BELİRLENMESİ

ÖZNUR CUMHUR
DOKTORA TEZİ
KİMYA MÜHENDİSLİĞİ ANABİLİM DALI

DANIŞMANI
DOÇ. DR. MAHMUT ŞEKER
II. DANIŞMAN
PROF. DR. HASAN SADIKOĞLU

GEBZE
2015

GEBZE TEKNİK ÜNİVERSİTESİ	**DOKTORA JÜRİ ONAY FORMU**

GTÜ Fen Bilimleri Enstitüsü Yönetim Kurulu'nun 24../06../2015. tarih ve 2015/.39.. sayılı kararıyla oluşturulan jüri tarafından 09/07/2015 tarihinde tez savunma sınavı yapılan Öznur CUMHUR'un tez çalışması Kimya Mühendisliği Anabilim Dalında DOKTORA tezi olarak kabul edilmiştir.

JÜRİ

ÜYE
(TEZ DANIŞMANI) : Doç. Dr. Mahmut ŞEKER

ÜYE : Prof. Dr. Hüsnü Yıldırım ERBİL

ÜYE : Doç. Dr. Zehra Sibel ÖZİLGEN

ÜYE : Prof. Dr. Hasan SADIKOĞLU

ÜYE : Prof. Dr. Fatma KARACA ALBAYRAK

ONAY

Gebze Teknik Üniversitesi Fen Bilimleri Enstitüsü Yönetim Kurulu'nun
...../...../..... tarih ve ...../..... sayılı kararı.

İMZA/MÜHÜR

SUMMARY

Freeze-drying is an attractive process to produce high quality dehydrated food products. In this work, a mathematical model that describes heat and mass transfer in freeze-drying process was constructed for the freeze-dried turkey breast meat and solved in order to describe quantitatively the dynamic behavior of the primary and secondary drying stages of the freeze-drying in trays. The model equations were solved using orthogonal collocation based on polynomial approximation-Jacobi method. Experimental results were obtained for the freeze-drying of meat by using a pilot freeze-dryer. Some parameters such as weight fraction of bound water, thermal conductivity of dried layer, Knudsen diffusivity for water vapor, film thermal conductivity and desorption rate constant of bound water for secondary drying stage that are difficult to measure directly were determined by fitting experimental data with the mathematical model using non-linear least square method of Levenberg-Marquardt algorithm of MATLAB. By using new estimated parameters in the dynamic mathematical model the duration of primary and secondary drying stages for 12.4 mm thick turkey breast meat slabs were found to be 11.0 h, 17 h, respectively. The mathematical model was validated with data obtained by freeze-drying of different thickness (14.5 mm) of turkey breast meat. The comparison of the theoretical results with the experimental data shows that the agreement between the experimental data and the theoretical results is good.

Key Words: Freeze-drying Process, Dynamic Transport Modeling, Parameter Estimation, Turkey Breast Meat.

ÖZET

Yüksek kalitede kurutulmuş gıda maddesi elde etmek için dondurarak kurutma en etkili prosestir. Bu çalışmada hindi etinin dondurarak kurutulması için enerji ve kütle eşitliklerine dayanan matematiksel model oluşturulmuş ve tepsili dondurarak kurutmanın birinci ve ikinci kurutma safhalarına ait dinamik davranışları tanımlamak için çözülmüştür. Model denklemleri polinom yaklaşımı-Jacobi yöntemine dayalı olan ortogonal kollokasyon metodu kullanılarak çözülmüştür. Deneysel sonuçlar pilot dondurarak kurutucuda etin dondurarak kurutulmasıyla elde edilmiştir. Bağlı suyun kütle fraksiyonu, kurumuş bölgedeki ısıl iletkenlik, su buharı Knudsen difüzyon katsayısı, film termal iletkenliği ve ikinci kurutma safhasındaki bağlı suyun desorpsiyon hız sabiti gibi direkt olarak ölçülmesi zor olan parametreler temeli en küçük kareler metoduna dayanan MATLAB Levenberg-Marquardt algoritması kullanılarak matematiksel modelin deneysel verilerle örtüşmesiyle belirlenmiştir. Modelde yeni elde edilen parametreler kullanılarak 12.4 mm kalınlığındaki hindi eti için birinci ve ikinci kurutma süreleri sırasıyla 11.0 saat, 17.0 saat olarak bulunmuştur. Matematiksel model farklı kalınlıktaki hindi göğüs etinin (14.5 mm) dondurarak kurutulmasıyla elde edilen verilerle doğrulanmıştır. Deneysel verilerle teorik sonuçların karşılaştırılması deneysel ve teorik sonuçlar arasındaki uyumun iyi olduğunu göstermektedir.

Anahtar Kelimeler: Dondurarak Kurutma Prosesi, Dinamik Taşınım Modelleme, Parametre Tahmini, Hindi Göğüs Eti.

ACKNOWLEDGEMENTS

I would like to express my deepest gratitude to my supervisors Prof. Dr. Hasan SADIKOĞLU and Assoc. Prof. Dr. Mahmut ŞEKER for their guidance, advice, critism and insight throughout the research.

I would like to thank thesis monitoring committee member Assoc. Prof. Dr. Zehra Sibel ÖZILGEN for her valuable comments, advice and kindness. I would also like to thank my thesis jury members: Prof. Dr. Hüsnü Yıldırım ERBİL and Prof. Dr. Fatma KARACA ALBAYRAK for their precious time. I want to express my thanks to research assistants Meral YILDIRIM YALÇIN and Ebubekir Sıddık AYDIN for all their help.

I want to thank all my friends who were with me during doctoral studies. Their support, friendship and encouragement are highly appreciated.

Finally, I would like to thank my parents for their love and support over the years and for encouraging me to pursue my dreams.

TABLE of CONTENTS

LIST of ABBREVIATIONS and ACRONYMS

Abbreviations and Acronyms		**Explanations**
α	:	Thermal diffusivity
ΔHs	:	Enthalpy of sublimation of frozen water
ΔHv	:	Enthalpy of vaporization of bound water
ε	:	Voidage fraction
μ_{mx}	:	Viscosity of vapor phase in the pores
ρ	:	Density
σ	:	Stefan Boltzmann constant
C_{0l}	:	Constant dependent only upon structure of porous medium and giving relative D'Arcy flow permeability
C_l	:	Constant dependent only upon structure of porous medium and giving relative Knudsen flow permeability
C_2	:	Constant dependent only upon structure of porous medium and giving the ratio of bulk diffusivity within the porous medium to the free gas bulk diffusivity
C_p	:	Heat capacity
C_{sw}	:	Weight fraction of bound water in dried layer
$D_{w.in}$	:	Free gas mutual diffusivity in a binary mixture of water vapor and inert gas
$D^o_{w.in}$	:	$D_{w.in}\,P$
F	:	View factor of the platen with the sample
f (T_x)	:	Water vapor pressure-temperature functional form
k	:	Thermal conductivity
k_1	:	Bulk diffusivity constant $k_1 = C_2 D^o_{w,in} K_w / (C_2 D^o_{w,in} + K_{mx} P)$
k_2, k_4	:	Self diffusivity constant $k_2 = k_4 = (K_w K_{in} / (C_2 D^o_{w,in} + K_{mx} P)) + (C_{01}/\mu_{mx})$
k_3	:	Bulk diffusivity constant $k_3 = C_2 D^o_{w,in} K_{in} / (C_2 D^o_{w,in} + K_{mx} P)$
k_d	:	Desorption rate constant of bound water
k_f	:	Film thermal conductivity

K_{in}	:	Knudsen diffusivity of inert gas, $K_{in} = C_1(RT_I/M_{in})^{0.5}$
K_{mx}	:	Weighted mean Knudsen diffusivity for binary gas mixture, $K_{mx} = y_W K_{in} + y_{in}K_w$
K_w	:	Knudsen diffusivity for water vapor, $K_w = C_1(RT_I/M_w)^{0.5}$
L	:	Sample thickness
M	:	Molecular weight
N	:	Mass flux
N_t	:	Total flux, $N_t = N_w + N_{in}$
P	:	Total pressure in dried layer
q	:	Heat flux
R	:	Universal gas constant
t	:	Time
T	:	Temperature
T_g'	:	Glass transition temperature
T_{gs}	:	Glass transition temperature of dry solid
T_{gw}	:	Glass transition temperature of water
T_m'	:	End point of freezing temperature
T_u	:	Eutectic temperature
V	:	Velocity of interface
x	:	Space coordinate of distance along the height of the material in the tray
X	:	Position of moving interface in the material
W	:	Mass fraction
WM	:	Amount of water
y	:	Mole fraction
Superscripts		
°	:	Initial value at time zero
Subscripts		
I	:	Dried region
II	:	Frozen region
a	:	Ash
b	:	Bound water
e	:	Effective value

f	:	Film
fa	:	Fat
i	:	Ice
in	:	Inert
L	:	Value at x=L
LP	:	Lower plate
m	:	Melting
mx	:	Mixture
o	:	Surface value
p	:	Protein
s	:	Solid
scor	:	Scorch
t	:	Theoretical
UP	:	Upper plate
w	:	Water vapor
exp	:	Experimental
X	:	Interfacial value

LIST of FIGURES

LIST of TABLES

1. INTRODUCTION

In the early 1960s, the freeze-drying of food was first welcomed world-wide as a new method of food preservation. In the following years, scientific and technical presumptions were the subject of many studies, to produce freeze-dried food for long term storage [Oetjen and Haseley, 2004]. The freeze-drying process is used for drying and preserving a number of food products, including meats, fruits, vegetables, instant coffee and tea products. Currently, freeze-dried foods increasingly take part in the international market.

The most remarkable characteristic of freeze-drying is the high quality of the dehydrated foods. Freeze-dried foods are maintained at much lower processing temperature than other drying process. The drying at low temperature is also good at retaining volatile flavor and aroma compounds in comparison to high temperature drying process. The low processing temperatures, the relative absence of liquid water and the rapid transition of any local region material being dried from a fully hydrated to a nearly completely dehydrated state minimize the degradative reactions such as enzymatic reactions, protein denaturation and non enzymatic browning. Freeze-dried foods are light in weight and can be stored at room temperature for long time. Another advantage of freeze-drying for foods is the effect of the ice structure in minimizing shrinkage of the product. The reduce shrinkage results in a porosity which enables rapid and nearly complete rehydration [King and Labuza, 1970], [Stapley, 2008], [Hua et al., 2010].

Despite the excellent quality of food products, freeze-drying process is not widely used in the food industry due to its high investment and operating costs. High operating costs of freeze-drying are related to the long processing times caused by the necessity of operating under high vacuum and at a very low temperature [Hua et al., 2010], [Ratti, 2001]. It is quite apparent that the cost of freeze-drying is a function of processing time and the high cost can be lowered by reducing duration of freeze-drying. This requires a precise understanding of simultaneous heat and mass transfer occurring during freeze-drying stages.

Freeze-dried meat products are popular in mountaineering, camping, military, baby food, astronaut rations and other instant meals [Stapley, 2008]. There are two basic types of studies related to freeze-dried meat: Experimental studies which

investigate the effect of the change of process conditions on the properties of meat and studies concentrating on the mathematical modeling in which the transport properties of the meat is calculated in terms of its physical structure. In particular, we are interested in modeling of heat and mass transfer for the freeze-drying of meat product.

Heat and mass transfer model for the freeze-drying of poultry meat was first developed by [Sandall et al., 1967]. Their model was based on Uniformly Retreating Ice Front (URIF). The model predicted the drying times to remove 60-90 % percent of the water. URIF model can only be used to explain the sublimation. This model is simple, but it cannot describe the dynamic behavior of primary and secondary drying stages in freeze-drying process. During removal of the last 10-35% of the water, the drying rate slows and the actual time is considerably greater than the predicted for this period. [Liapis and Litchfield, 1979] developed a mathematical model to describe the non-steady state heat and mass transfer operations during freeze-drying process. In their study, [Liapis and Litchfield, 1979] assumed that the heat to the slab material comes only from above and desorption of unfrozen water is not taken into consideration. Their model was also compared with URIF model and showed better accordance with data than the URIF model showed with it but merely when the removal of free water into consideration. [Litchfield and Liapis, 1979] presented another model to represent dynamic behavior of the primary drying stage of turkey meat freeze-drying in trays. Unlike the previously described models, both sublimation of ice and desorption of unfrozen water in dried region were formulated simultaneously. The model of [Litchfield and Liapis, 1979], however, is not complete, because does not account the heat input from the bottom surface of the material being dried, which is the case for most of the industrial freeze dryers. Furthermore, the present model does not predict the dynamic behavior of the secondary drying stage which takes much longer time compare to the primary drying stage. It just predicts the dynamic behavior of the primary drying stage. In 1982, Litchfield and Liapis proposed a model to manipulate the radiator energy output and the total pressure in the drying chamber in order to minimize the time required to get a fixed amount of residual water in the turkey meat at the end of the primary drying stage [Litchfield and Liapis, 1982]. [Litchfield et al., 1981] studied the cyclical pressure freeze-drying model to investigate the effect of cyclical pressure on drying

times in turkey meat. The study found that the best of the cyclical pressure policies was not as good as an optimal constant pressure policy.

There are interests to reduce the rate of salt content in process food products. Current regulations were made to reduce the rate of salt amount in process food products especially in meat products like bacon, pastrami etc. Conventional drying methods of low-salted meat products increase the risk of microbial spoilage during processing. Therefore, freeze-drying method seems to be a promising dehydration method to reduce the risk of spoilage in low-salted meat products. In this sense, this thesis aims to contribute to the advancement of the freeze-dried low salted meat products.

This research analyses fundamental heat and mass transfer mechanism of freeze-drying of turkey breast meat. Mass flow through the dried layer is modeled using a combination of the dusty gas model that does not require detailed information about the structure of the porous matrix of the dried layer such as porosity, tortuosity, pore size distribution and pore connectivity. The dusty gas model was used to describe mass transport in other foods such as coffee and milk [Boss et al., 2004], [Sadikoglu and Liapis, 1997].

The modified dynamic mathematical model based on the conservation of the mass and energy constructed and solved to represent the primary and secondary drying stages of freeze-drying of turkey breast meat. Some transport parameters and physical properties that characterize freeze-drying of turkey breast meat were determined by fitting experimental data with the mathematical model. The theoretical results that obtained with the best fitted parameters were compared with the experimental data that were obtained from freeze-drying of turkey breast meat by using a pilot scale freeze-drier. Also, the mathematical model presented in this work was validated with data obtained by freeze-drying of different thickness (14.5 mm) of turkey breast meat.

2. FREEZE-DRYING PROCESS

2.1. Principles of Freeze-Drying

Freeze-drying also known as lyophilization, or cryodesiccation is a separation process where frozen solvent content, particularly water, removed from the material being freeze dried by sublimation under reduced pressure [Liapis and Bruttini, 2006]. Freeze-drying process involves three essential stages: freezing, primary drying, secondary drying. These different physical phenomena take place, as depicted in water phase diagram (Figure 2.1) [Lopez-Quiroga et al., 2012].

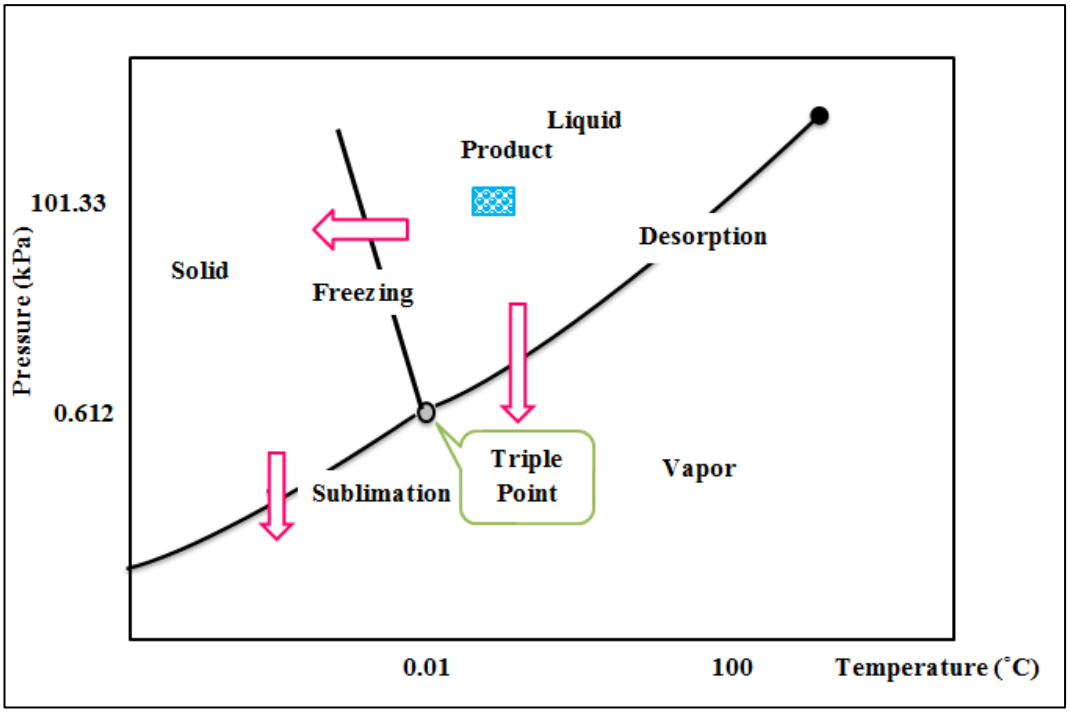

Figure 2.1: Freeze-drying phenomena represented on phase diagram of water.

If a product at the pressure and temperature corresponding to ambient conditions should first be frozen by decreasing its temperature, then the water vapor pressure should be lowered below the pressure corresponding to the triple point and finally some heat should be supplied to help the ice to convert into vapor by sublimation [Ratti, 2012]. Desorption of nonfreezable water occurs during primary and secondary drying stage.

2.2. Freezing Stage

Freezing is the first step in the freeze-drying process. The liquid formulation in the product is cooled until ice starts to nucleate, which is followed by ice growth during the freezing stage. This results in the separation of most of the water into ice crystals from a matrix of glassy and/or crystalline solutes [Kasper and Friess, 2011]. While simple in concept, the freezing stage will be shown to be perhaps the most complex step in the process. Its effect on the drying process is paramount, and it can impact the properties of the final product [Jennings, 2008]. The characteristic of frozen matrix influence the primary and secondary drying rate and product recrystallization [Gieseler, 2004].

In practice, materials exhibits one of two different types of freezing behavior. (a) The liquid phase suddenly solidifies at a temperature that depends on the nature of solids in the sample (eutectic formation) or (b) The liquid phase doesn't solidify, but rather it becomes more and more viscous until it finally takes the form of a very stiff substance and becomes highly viscous liquid (glass formation) or amorphous state [Liapis and Bruttini, 2006].

Foods are multiphase with complex structure. Supplemented phase diagram (Figure 2.2) represents different phase boundaries in a food as a function of temperature water or solids content and temperature. It also simplifies the discussion of freeze-drying process. In Figure 2.2 the freezing line (ABC) and solubility line (BE) are shown in relation to the glass transition line (FDG). The freezing and solubility lines intersect at the eutectic point B, which is defined as the lowest temperature at which is liquid phase can exist in equilibrium with ice crystals. The point D (X_s' and T_g') lower than T_m' (point C) is a characteristic transition (maximal freeze concentration condition) in the state diagram defined as the intersection of the vertical line from T_m' to the glass line [Rahman, 2006], [Searles, 2010].

The initial freezing point of food is slightly lower than the freezing point of pure water because of dissolved substances in the moisture in the food. The presence of substances suppresses the beginning of the freezing process. Removing heat from the food initially causes it to cool a few degrees below the equilibrium freezing point without crystallization, is said to be super cooling. A few degrees of sub-cooling are required to initiate nucleation and crystallization of ice crystals [Ashrae, 2006],

[Stapley, 2008]. The degree of supercooling depends on the physical properties of the sample and process conditions [Sadikoglu et al., 2006]. In foods the degree of supercooling is much smaller than in pure water because of heterogeneous ice nucleation [Nesvadba, 2008]. The formation of an ice results in an increasing concentration of the remaining solution in the food and the freezing point temperature decreases steadily. The solution approaches the glass transition line and the solution reaches end point of freezing curve where further cooling will no longer change the concentration of solution [Singh and Sarkar, 2005], [Rahman, 2006]. At temperature higher than T_m' freeze concentration will stop at lower concentration due to insufficient sub-cooling [Stapley, 2008]. Some of the water in food remains in the solution and is unavailable for freezing. The water content at point C or D is considered as the un-freezable water (1-Xs'). Un-freezable water includes both un-crystallized free water and bound water attached to the solids matrix [Singh and Sarkar, 2005], [Rahman, 2006]. About 10% of the water content of meat does not appear to freeze, and it is generally assumed to be too tightly bound to protein, while the remaining 90% of the water content is freezable [James and James, 2002].

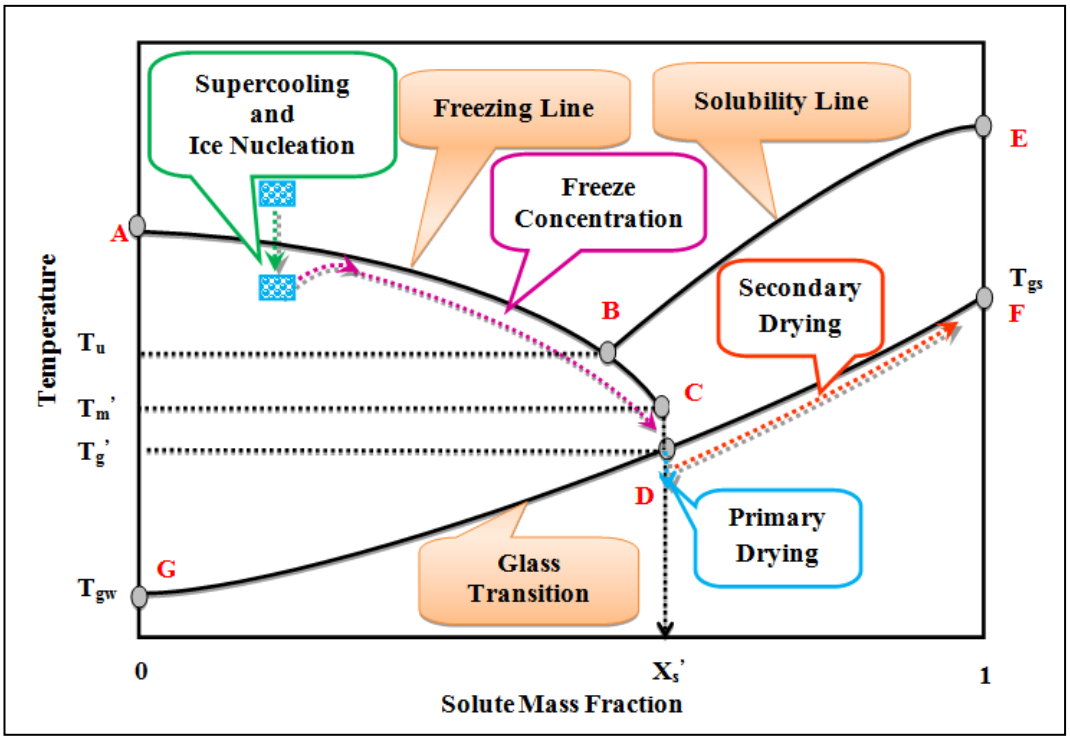

Figure 2.2: Supplemented phase diagram and freeze diagram process for foods.

The ice crystals formed during the freezing stage determine the size and shape of the pores, the pore size distribution and pore connectivity of the porous network of the dried layer formed by sublimation of the frozen water during the primary drying stage. This porous structure of the dried product influences the parameters that characterize the heat and mass transfer rates in the dried product during the primary and secondary drying stages. Pore structure also affects the rehydration behavior, appearance and density of the freeze-dried product [Sadikoglu et al., 2006], [Stapley, 2008]. If smaller and more discontinuous ice crystals are formed upon quick freezing, there is a greater diffusion resistance for the transport of water vapor during drying process. If fewer large ice crystals are formed during slow freezing that result in small diffusion resistance and higher water vapor mass transfer rates in the pores of the dried product [Sadikoglu et al., 2006].

2.3. Primary Drying Stage

In the primary drying stage, the water vapor pressure should be lowered below the pressure corresponding to the triple point and requisite amount of energy should be supplied for the removal of frozen water by sublimation and removal of unfrozen water by desorption in the dried layer [Liapis and Bruttini, 2006]. During the primary drying stage, as the ice sublimes, the sublimation interface which started at the upper surface passes inward and porous shell of dried material remains. The amount of bound water removed in primary drying stage is very small compared with sublimation. But the desorption process in the dried layer could affect the amount of heat that arrives at the sublimation interface, and therefore it could affect the velocity of the moving sublimation interface. When all ice sublimated and the sublimation interface is completely lost, and the primary drying stage ends [Liapis et al., 1996].

The driving force for sublimation depends essentially on the difference in vapor pressure between the moving interface and the cold surface of the condenser [Mellor, 1978]. The energy required for sublimation and desorption of bound water can be supplied by an adequate heating during primary drying [Lombrana, 2008]. In general, the upper surface heat is delivered to the exposed surface of the dried layer by thermal radiation and then travels through the dried layer to the sublimation interface, mainly by conduction. The bottom surface heat input of the frozen layer is supplied by heating plate and is transferred by conduction to the sublimation

interface through the frozen layer of sample. The water vapor released also travels through the dried layer, from the sublimation front to the surface and from there to the condenser. Freeze-drying involves simultaneous heat and mass transfers which have to be taken into account when models are developed [Berk, 2009], [Daraoui et al., 2010].

Critical product features during primary drying are the product temperatures in the dried and frozen layers, the values of the concentration of moisture in the dried layer, the velocity and temperature of the moving interface, the geometrical shape of the moving interface and the duration of the primary drying stage. The goal in primary drying is to find operating conditions for the freeze-dryer that would minimize the duration of primary drying by maximizing the velocity of the moving interface. The structural and chemical stability in the dried layer of the product are functions of the temperature and concentration of moisture at every point in the dried layer [Liapis et al., 1996].

The amount of heat cannot be increased freely because the temperatures of the dried and frozen layer below certain prefixed levels, assuring good quality in the dehydrated product. One of the constraints is maximum allowable temperature value for the dried layer, called scorch temperature, T_{scor}. This maximum temperature that tolerate without loss of bioactivity, color change, the possibility for degradative chemical and biochemical reactions to occur and structural deformation in the dried layer [Liapis and Bruttini, 2006], [Lombrana, 2008]. Scorch temperatures for most foodstuffs are higher than 40°C [Ratti, 2012]. The scorch temperature for turkey meat is 60 °C, seen in Table 4.2 [Litchfield and Liapis, 1982].

The maximum temperature value for the frozen layer is another constraint during the primary drying stage. If the material has a eutectic form, the heating temperature should be kept lower than the eutectic temperature. Otherwise melting in the frozen layer can occur. The melting at the sublimation interface, or any melting that would occur in the frozen layer, can cause gross material faults such as puffing, shrinking, and structural topologies filled with liquid solution [Liapis and Bruttini, 2006]. The melting point of foods is around -10 °C because it depends on the amount of bound water, which is similar for a great variety of foods [Lombrana, 2008]. If the material has a solute system which does not crystallize but remains amorphous, the temperature of the frozen layer cannot exceed the collapse temperature, T_c. This makes the product collapse with a loss of its structure in the dried region. Collapse

affects aroma retention, caking, and stickiness rehydration capacity and final moisture of the product [Pikal and Shah, 1990], [Welti-Chanes et al., 2005]. The collapse temperatures are much lower for products having a weak structure, such as juices [Ratti, 2012].

2.4. Secondary Drying Stage

The secondary drying stage, also called desorption drying, involves the removal of unfrozen water (bound water) in the dried layer of the product. The unfrozen water may be adsorbed on the surface of the crystalline product or is in the solute phase either as hydrate water in a crystalline hydrate or dissolved in an amorphous solid to form a solid solution [Pikal et al., 1990]. At the beginning of the secondary drying stage, there is no longer moving sublimation interface and frozen layer. For the bound water to be removed, it must first diffuse from within the solid material to the surface of a pore. At this point, the water desorbs from the surface. The rate of diffusion and desorption is determined by the temperature of the material and the amount of moisture in the pore [Dolan, 1998].

The heat of desorption is supplied by radiation from the top of the sample through the gas phase and by heating plates at the bottom surface of the material being freeze-dried. The heat input from top and bottom surfaces of the sample is transferred by the conduction to the porous dried layer [Sadikoglu et al., 2006].

The goals in secondary drying are to find operating conditions for the freeze-dryer that would minimize the duration of the secondary drying stage without loss of structural and chemical stability of the product during drying and would provide at the end of the secondary drying stage a desirable concentration profile of moisture. The moisture content within the product is related to the temperature profile in the dried layer [Liapis et al., 1996]. The temperature of the sample must not exceed T_{scor} in order not to have significant losses in structural and chemical stability and bioactivity of the product [Sadikoglu et al., 2006].

3. MATERIALS AND METHODS

3.1. Sample Analysis

Turkey breast meat was used for experiment. Bolca (Bolu, Turkey) brand's turkey breast meat was bought from a local store and was kept at 4 ˚C under refrigeration until the usage. Initial moisture content of turkey meat product was measured on a separate sample by oven drying method. Approximately 1.5-2 g of meat was put in pre-weighed Petri dishes, dried in oven at 105°C until the constant weight was reached, cooled down in the desiccator and then reweighed [Wiklund et al., 2010]. The moisture content of sample is calculated using the following equation:

$$\%\text{moisture} = \frac{m_2 - m_3}{m_2 - m_1} x100 \tag{3.1}$$

- m_1 : tare of dish (g)
- m_2 : weight of wet meat +tare (g)
- m_3 : weight of dry meat + tare (g)

3.2. Freeze-Drying Analysis for Turkey Meat

Mainly, two sets of experiments were designed to obtain data for freeze-drying of turkey breast meat. The first set of experiment was conducted to collect sample temperature measurements data while the second set of experiment was conducted to collect weight loss data. In the freeze-drying experiments, a pilot scale freeze dryer (VirTis Ultra 25 Super XL, New York, ABD) that allow to set the heating (or cooling) plate temperature from 233 to 333 K and capable of supplying vacuum as low as 5 Pa was used (Figure 3.1). For each freeze-drying experiment, 4 samples (35.88±1.6 g pre-weighed) were placed into a tray of the freeze dryer, and then the temperature of the plates was set to its minimum value of 233 K for four hours to completely freeze the sample. The drying chamber pressure was set to 10 Pa and kept constant during entire freeze-drying process. When the drying chamber pressure reached its set value of the 10 Pa then the thermostat of the heating plates was set at

293.15 K for both primary and secondary drying stages. The temperature of the condenser was set to its minimum value of 203.15 K and kept constant during entire drying process to enhance water vapor mass flux from sample to ice condenser.

Figure 3.1: VirTis Ultra 25 Super XL Pilot Lyophilizer.

3.2.1. Sample Preparation

The breast meat was prepared for freeze-drying by removing fat parts and slicing into 12.4 and 14.5 mm thickness, 73.0 mm length and 33.0 mm width. The samples with thickness of 14.5 mm were used for validation of the mathematical model. All measures of position and distances were determined by using an Electronic Digital Caliper (Fred Fowler Co., Newton, MA). Heat flow direction was perpendicular to the orientation of the meat fiber (Figure 3.2).

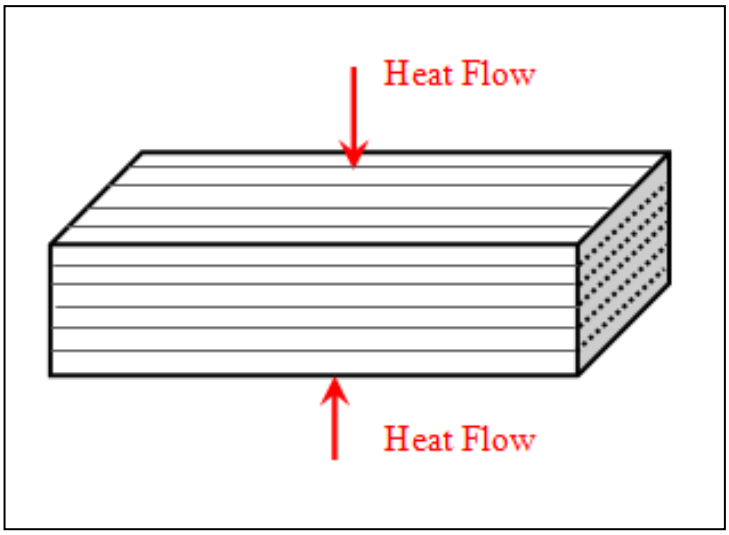

Figure 3.2: Fiber configurations in turkey breast meat sample, fiber directions perpendicular to heat flow.

3.2.2. Temperature Measurement

The temperature profiles during the freeze-drying were obtained by placing four thermocouples into two different samples in contact with surface and geometric center point of the products (Figure 3.3). The thermocouple insertion was performed into fresh meat samples before freezing. Then the meat products with the inserted thermocouple were frozen and freeze-dried. During freeze-drying, temperature variations were recorded by a digital data logger, which was directly linked to the computer and temperature acquisition was done at one minute intervals.

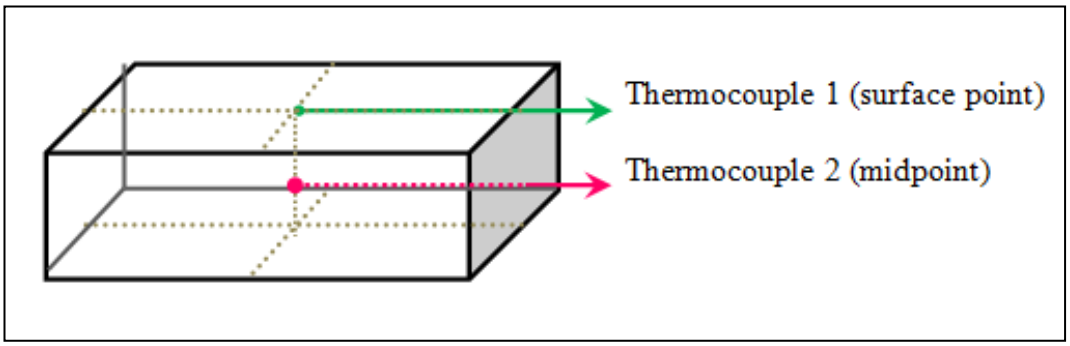

Figure 3.3: Thermocouple locations on sample.

3.2.3. Moisture Content Measurement

Four meat samples were weighed and introduced into the freeze-dryer for process application. The duration of the freeze-drying was calculated from the moment when the heating system started. To calculate the amount of water that was eliminated, the samples were weighed every 2 hours until the constant weighing, using a Mettler Toledo Balance (PB 503 ± 0.001, Switzerland) before and after the freeze-drying operation.

3.3. Mathematical Description of Freeze-Drying

A schematic representation of the meat slab on a tray during freeze-drying is given in Figure 3.4. A mathematical model based on the material and energy balances equations was constructed according to existent model [Sadikoglu and Liapis, 1997]. For modeling purposes, the following assumptions were made [Millman et al., 1985], [Sadikoglu and Liapis, 1997], [Khalloufi, et al., 2005]:

- Only one dimensional heat and mass flows, normal to the interface and surfaces, are considered.
- Sublimation occurs at an interface parallel to, and at a distance X from the upper surface of the sample.
- The thickness of the interface is considered to be infinitesimal.
- A binary mixture of water vapor and inert gas flows through the dried layer.
- At the interface, the concentration of water vapor is in equilibrium with the ice.
- In the porous region, the solid matrix and the gas are in thermal equilibrium.
- The frozen region is considered to be homogenous, of uniform thermal conductivity, density and specific heat and to contain a negligible proportion of dissolved gases.
- Thermal resistance of tray material to heat transfer is considered to be negligible.
- The magnitude of heat transfer to the vertical sides of the tray, q_{III}, is negligible when compared to the magnitude heat input to material being freeze-dried from the top and bottom surfaces, q_I and q_{II}, respectively.

• Shrinkage of meat product is not considered. If necessary, the effect of meat shrinkage on the internal and external mass and heat transfer mechanism of the freeze-drying process can be estimated using model of Sadikoglu et al. [1999].

The dynamic behavior of the primary and secondary drying stages of the freeze-drying process is described in the following section.

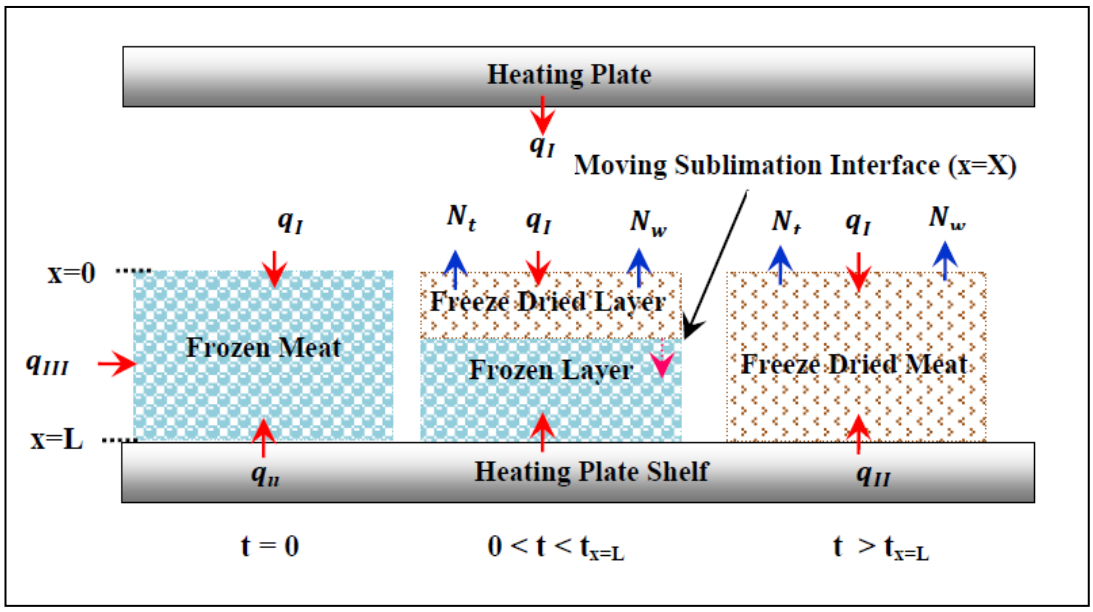

Figure 3.4: Schematic representation of a meat product on tray during freeze-drying at initial time (t=0), during primary drying ($0 < t < t_{x=L}$) and during secondary drying ($t > t_{x=L}$).

3.3.1. Primary Drying Stage

In the primary drying stage sublimation and desorption occurs as a result of heat conducted to the sublimation interface through the dried (I) and frozen layers (II). The heat transfer in dried and frozen layers is as follows:

$$\frac{\partial T_I}{\partial t} = \alpha_{Ie}\frac{\partial^2 T_I}{\partial x^2} - \frac{c_{pg}}{\rho_{Ie}c_{pIe}}\left(\frac{\partial (N_t T_I)}{\partial x}\right) + \frac{\Delta H_v \rho_I}{\rho_{Ie}c_{pIe}}\left(\frac{\partial C_{sw}}{\partial t}\right); \qquad 0 \le x \le X, \quad t>0 \tag{3.2}$$

$$\frac{\partial T_{II}}{\partial t} = \alpha_{II}\frac{\partial^2 T_{II}}{\partial x^2}; \qquad X \le x \le L, \quad t>0 \tag{3.3}$$

where $\alpha_{Ie} = k_{Ie}/\rho_{Ie}c_{pIe}$ and $\alpha_{II} = k_{II}/\rho_{II}c_{pII}$. Total mass flux ($N_t$) is equal to sum of inert gas flux and water vapor flux ($N_t = N_w + N_{in}$) [Liapis and Bruttini, 2006].

At the beginning of the freeze-drying process, the temperature of sample is uniform therefore initial conditions can be specified for the heat transfer equations as follows [Sadikoglu and Liapis, 1997]:

$$T_I = T_{II} = T_X = T^0; \qquad 0 \le x \le L, \quad t=0 \tag{3.4}$$

Heat input to the upper surface of the material ($x = 0$) being freeze-dried occurs by radiation then transferred to the moving interface by conduction.

$$q_I = -k_{Ie}\frac{\partial T_I}{\partial x}|_{x=0}; \qquad x=0, \ t>0 \tag{3.5}$$

$$q_I = \sigma F\left(T_{up}^4 - (T_I(t,0))^4\right); \qquad x=0, \ t>0 \tag{3.6}$$

Applying conservation of the energy principle for infinitesimal moving interface where the temperature of dried (I) and frozen (II) layer are both equal to each other, equation (3.7) can be obtained:

$$k_{II}\frac{\partial T_{II}}{\partial x}\Big|_{x=X} - k_{Ie}\frac{\partial T_I}{\partial x}\Big|_{x=X} + V\left(\rho_{II}C_{pII}T_{II}\Big|_{x=X} - \rho_I C_{pI}T_I\Big|_{x=X}\right) + N_t C_{pg}T_x = -\Delta H_s N_t; \qquad x = X, \quad 0<t\le t_{x=X} \tag{3.7}$$

$$T_I = T_x = T_{II}; \qquad x=X, \quad 0<t\le t_{x=X} \tag{3.8}$$

In equation (3.7), the first and second term represent heat input to the moving interface through frozen (II) and dried (I) layers, respectively by conduction. The third term represents the heat input to the interface by convection while the fourth term represents the amount of heat that leaves the moving interface as water vapor and inert gas. The right side of the equation (3.7) represents the amount of energy required for sublimation of frozen water at interface.

Heat input to the material being freeze-dried from bottom surface can take place by radiation or conduction depending on the design of freeze dryer. Uploaded heat from the bottom surface of the material transferred to moving interface through frozen layer by conduction.

$$q_{II} = k_{II} \frac{\partial T_{II}}{\partial x} \Big|_{x=L}; \qquad x=L, \ t > 0 \tag{3.9}$$

For radiation only at $x = L$,

$$q_{II} = \sigma F\left(T_{Lp}^4 - (T_{II}(t,L))^4\right); \qquad x=L, \quad t > 0 \tag{3.10}$$

For a thin film between the frozen material and a lower plate at $x = L$,

$$q_{II} = k_f\left(T_{LP} - T_{II}\,(t, L)\right); \qquad x=L, \quad t>0 \tag{3.11}$$

The material balance equations for the inert gas and water vapor flowing through the dried layer are as follows [Sadikoglu and Liapis, 1997]:

$$\frac{1}{R}\frac{\partial}{\partial t}\left(\frac{P_{in}}{T_I}\right) = -\frac{1}{M_{in}\varepsilon}\frac{\partial N_{in}}{\partial x}; \qquad 0 \le x \le X \tag{3.12}$$

$$\frac{1}{R}\frac{\partial}{\partial t}\left(\frac{P_w}{T_I}\right) = -\frac{1}{M_w\varepsilon}\frac{\partial N_w}{\partial x} - \frac{\rho_I}{M_w\varepsilon}\frac{\partial C_{sw}}{\partial t}; \qquad 0 \le x \le X \tag{3.13}$$

The term $\partial Csw/\partial t$ in equation (3.2) and equation (3.13) accounts for the change in concentration of sorbed or bound water with time and in this study following rate mechanism is considered. The parameter k_d represents the desorption rate constant of the linear rate mechanism that could be used to describe the desorption of bound water.

$$\frac{\partial C_{sw}}{\partial t} = -k_d C_{sw} \tag{3.14}$$

In this mathematical model, water vapor (sublimated and desorbed) and inert gas flows through porous dried layer. Description of mass transfer in porous layer is studied according to the dusty gas model. The very important practical advantage of the dusty-gas model is that it does not require detailed information about the structure of the porous matrix of the dried layer such as porosity, tortuosity, pore size distribution and pore connectivity. All the information of pore structure characteristics is in the structural parameters C_{01}, C_1 and C_2 that characterize the mechanism of intraparticle convective flow, Knudsen diffusion and bulk diffusion, respectively. Gas transport through porous media can be divided into three independent mechanisms, as follows [Mason and Malinauskas, 1983]:

- Free molecule or Knudsen diffusion, in which the gas density is so low that collisions between molecules can be ignored compared to collisions of molecules with the walls of the porous medium.
- Viscous flow or convective flow, in which the gas acts as a continuum fluid driven by a pressure gradient, and molecule-molecule collisions dominate over molecule-wall collisions.
- Continuum diffusion, in which the different species of a mixture move relative to each other under the influence of concentration gradients, temperature gradients or external forces. Molecule-molecule collisions dominate over molecule- wall collisions.

Mass fluxes of water vapor and inert gas equations based on Dusty-gas model, N_w and N_{in} can be expressed as follows [Sadikoglu and Liapis, 1997]:

$$N_w = -\frac{M_w}{RT_I}\left(k_1\frac{\partial P_w}{\partial x} + k_2 P_w\left(\frac{\partial P_w}{\partial x} + \frac{\partial P_{in}}{\partial x}\right)\right) \tag{3.15}$$

$$N_{in} = -\frac{M_{in}}{RT_I}\left(k_3\frac{\partial P_{in}}{\partial x} + k_4 P_{in}\left(\frac{\partial P_w}{\partial x} + \frac{\partial P_{in}}{\partial x}\right)\right) \tag{3.16}$$

The initial and boundary conditions of material balance equations (3.12) and (3.13) and rate mechanism equation (3.14) are the following [Sadikoglu and Liapis, 1997].

$$P_w = P_w^{\circ}, \quad P_{in} = P_{in}^{\circ}; \quad 0 \leq x \leq X, \ t = 0 \tag{3.17}$$

$$C_{sw} = C_{sw}^{\circ}, \quad 0 \leq x \leq L; \ t = 0 \tag{3.18}$$

$$P_w = P_{wo}, \quad P_{in} = P_{ino} = P_o - P_{wo}; \quad x = 0, \ t > 0 \tag{3.19}$$

$$P_w = f(T_x); \quad x = X, \ 0 < t \leq t_{x=L} \tag{3.20}$$

$$\frac{\partial P_{in}}{\partial x}\Big|_{x=X} = 0; \quad x = X, \ 0 < t \leq t_{x=L} \tag{3.21}$$

The variable P_{wo} is the chamber water vapor pressure determined by the condenser design and assumed constant within the drying chamber. P_o is the total pressure ($P_o = P_{wo} + P_{ino}$) at the surface of dried layer and is usually considered to be approximately equal to the total pressure in the drying chamber [Sadikoglu and Liapis, 1997]. The transition zone from the frozen to dried layers where the sublimation of ice takes place is assumed to be in equilibrium with the temperature at the corresponding location. The vapor pressure at the sublimation interface equation (3.20) is obtained by means of the corresponding thermodynamic solid-vapor equilibrium function for water (can be seen in Table 4.2) depending on the sublimation temperature [Sadikoglu and Liapis, 1997], [Lombrana, 2008].

Equation (3.22) indicates that the difference between the rate of disappearance of mass of frozen layer and the rate of formation of mass of dried layer is equal to the vapor flow rate at the moving interface [Velardi and Barresi, 2008]. The material balance at the interface can be written as:

$$V = \frac{dX}{dt} = -\frac{N_w|_{x=X}}{\rho_{II} - \rho_{Ie}} \tag{3.22}$$

where position of interface is a function of time and the initial condition $X = 0$ at $t = 0$ [Sadikoglu and Liapis, 1997].

3.3.2. Secondary Drying Stage

When the primary drying stage ends, there is no frozen layer and thus there is no moving sublimation interface. The secondary drying stage involves the removal of bound (unfrozen) water [Liapis and Bruttini, 2006]. In the secondary drying stage, the thickness of the drying layer is equal to the thickness of the meat sample (L) and the energy balance in the layer is as follows [Sadikoglu and Liapis, 1997]:

$$\frac{\partial T_I}{\partial t}=\alpha_{Ie}\frac{\partial^2 T_I}{\partial x^2}-\frac{c_{pg}}{\rho_{Ie}c_{pIe}}\left(\frac{\partial(N_t T_I)}{\partial x}\right)+\frac{\Delta H_v \rho_I}{\rho_{Ie}c_{pIe}}\left(\frac{\partial C_{sw}}{\partial t}\right);\qquad 0\le x\le L,\quad t> t \tag{3.23}$$

The continuity equations are given by equations (3.12) and (3.13) while the equation for the removal of bound water is given by equation (3.14).

The functions $\gamma(x)$, $\delta(x)$, $\theta(x)$ and $v(x)$ provide the profiles of T_I, P_w, P_{in} and C_{sw} at the end of the primary drying stage. These profiles are obtained by solution of the model equations for the primary drying stage. They are the initial conditions of secondary drying and they are all functions of position x, as shown in the following equations.

$$T_I=\gamma(x);\qquad 0\le x\le L,\quad t=t_{x=L} \tag{3.24}$$

$$P_w=\delta(x);\qquad 0\le x\le L,\quad t=t_{x=L} \tag{3.25}$$

$$P_{in}=\theta(x);\qquad 0\le x\le L,\quad t=t_{x=L} \tag{3.26}$$

$$C_{sw}=v(x);\qquad 0\le x\le L,\quad t=t_{x=L} \tag{3.27}$$

At the surface, heat is transferred to the upper dried surface by radiation and heat is assumed to be transferred only by conduction within the product.

$$q_I = -k_{Ie} \frac{\partial T_I}{\partial x}\Big|_{x=0}; \qquad x=0, \quad t>t_{x=L} \tag{3.28}$$

$$q_I = \sigma F\left(T_{up}^4 - (T_I(t,0))^4\right); \qquad x=0, \quad t>t_{x=L} \tag{3.29}$$

$$q_{II} = k_{Ie} \frac{\partial T_I}{\partial x}\Big|_{x=L}; \qquad x=L, \quad t>t_{x=L} \tag{3.30}$$

The boundary conditions of material balance equations are given by the following expressions:

$$P_w = P_{wo}, \quad P_{in} = P_{ino} = P_o - P_{wo}; \qquad x=0, \quad t \geq t_{x=L} \tag{3.31}$$

$$\frac{\partial P_w}{\partial x}\Big|_{x=L} = 0; \qquad x=L, \quad t>t_{x=L} \tag{3.32}$$

$$\frac{\partial P_{in}}{\partial x}\Big|_{x=L} = 0; \qquad x=L, \quad t>t_{x=L} \tag{3.33}$$

3.4. Coordinate Transformation of the Model Equations

The numerical solution of the equations of the model is complicated because the interface separating the dried layer (I) and the frozen layer (II) region moves from the beginning to the end of the primary drying stage. Landau's transformation immobilizes the moving interface and transforms the problem of the freeze-drying process to a problem of fixed domain in which frozen and dried region is constant (Figure 3.5) [Sadikoglu, 1998].

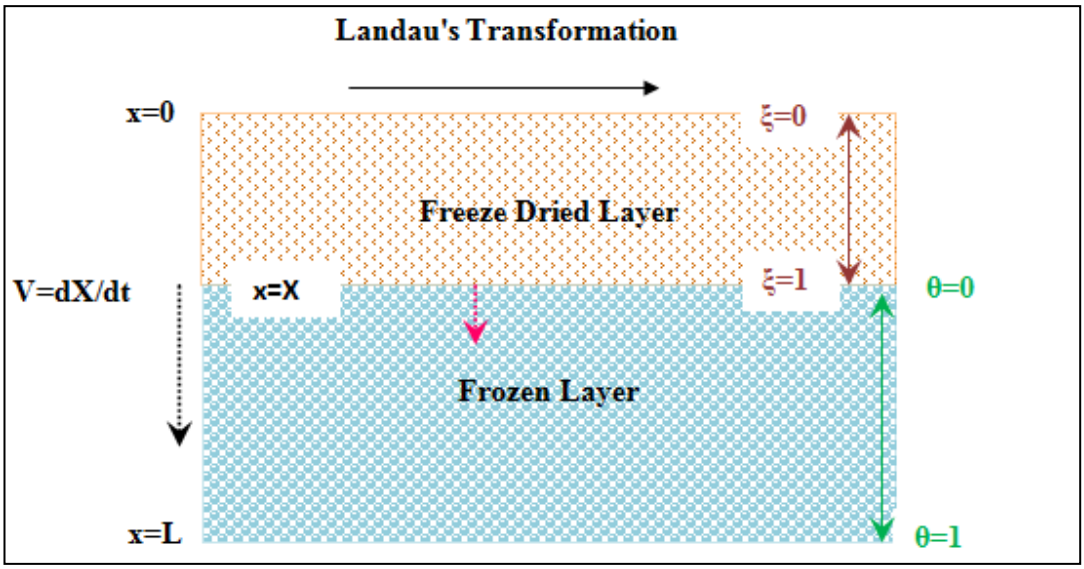

Figure 3.5: Scheme of the Landau's Coordinate Transformation.

The equations in the dried layer can be transformed from the (t,x) coordinate system to the (ϒ,ξ) coordinate system and the equation in the frozen layer can be transformed into the (ϒ,θ) system by following transformation equations.

$$\Upsilon = t \tag{3.34}$$

$$\xi = \frac{x}{X(t)}; \qquad 0 \le x \le X(t) \tag{3.35}$$

$$\theta = \frac{x - X(t)}{L - X(t)}; \qquad X(t) \le x \le L \tag{3.36}$$

ξ coordinate system selected for dried region:

$$\frac{\partial \Upsilon}{\partial x} = 0\,, \qquad \frac{\partial \Upsilon}{\partial \theta} = 0, \qquad \frac{\partial \Upsilon}{\partial t} = 1 \tag{3.37}$$

$$\frac{\partial \xi}{\partial t} = \frac{(0)X(t) - x\frac{\partial X(t)}{\partial t}}{X(\Upsilon)^2} = -\frac{x}{X(\Upsilon)^2}\frac{\partial X(t)}{\partial \Upsilon}\frac{\partial \Upsilon}{\partial t} = -\frac{\xi}{X(\Upsilon)}\frac{\partial X(t)}{\partial \Upsilon} \tag{3.38}$$

$$\frac{\partial \xi}{\partial x} = \frac{(1)X(\tau) - x(0)}{X(\tau)^2} = \frac{1}{X(\tau)} \tag{3.39}$$

$$\frac{\partial^2 \xi}{\partial x^2} = \frac{\partial}{\partial x}\left(\frac{\partial \xi}{\partial x}\right) = \frac{\partial}{\partial x}\left(\frac{1}{X(\tau)}\right) = 0 \tag{3.40}$$

θ coordinate system selected for frozen region:

$$\frac{\partial \theta}{\partial t} = \frac{-\frac{\partial X(\tau)}{\partial \tau}[L - X(\tau)] - [x - X(\tau)]\left[-\frac{\partial X(\tau)}{\partial t}\right]}{[L - X(\tau)]^2} = \frac{\frac{\partial X(\tau)}{\partial t}(x - L)}{[L - X(\tau)]^2} \tag{3.41}$$

By using equation (3.36) into equation (3.41) the following expression for $\partial\theta/\partial t$ is obtained:

$$\frac{\partial \theta}{\partial t} = \left[\frac{L(\theta - 1) + X(\tau)(1 - \theta)}{[L - X(\tau)]^2}\right]\frac{\partial X(\tau)}{\partial t} \tag{3.42}$$

$$\frac{\partial \theta}{\partial x} = \frac{(1)[L - X(t)] - [x - X(t)](0)}{[L - X(t)]^2} = \frac{1}{[L - X(t)]} \tag{3.43}$$

$$\frac{\partial^2 \theta}{\partial x^2} = \frac{\partial}{\partial x}\left(\frac{\partial \theta}{\partial x}\right) = \frac{\partial}{\partial x}\left(\frac{1}{[L - X(t)]}\right) = 0 \tag{3.44}$$

Temperature of the dried region (T_I) is function of time and space.

$$T_I = T_I(\tau, \xi) \Rightarrow dT_I = \left(\frac{\partial T_I}{\partial \xi}\right)_\tau d\xi + \left(\frac{\partial T_I}{\partial \tau}\right)_\xi d\tau \tag{3.45}$$

In order to obtain $\left(\frac{\partial T_I}{\partial t}\right)$ divides equation (3.45) by dt.

$$\frac{\partial T_I}{\partial t} = \left(\frac{\partial T_I}{\partial \xi}\right)_\tau \frac{\partial \xi}{\partial t} + \left(\frac{\partial T_I}{\partial \tau}\right)_\xi \frac{\partial \tau}{\partial t} \tag{3.46}$$

∂ζ/ ∂t=1. By using equation (3.38) into equation (3.46) the following expression for $\partial T_I/\partial t$ is obtained in the (ζ,ξ) coordinate system.

$$\frac{\partial T_I}{\partial t} = -\frac{\xi}{X(\zeta)}\frac{\partial X(t)}{\partial \zeta}\frac{\partial T_I}{\partial \xi} + \frac{\partial T_I}{\partial \zeta} \tag{3.47}$$

In order to obtain $\left(\frac{\partial T_I}{\partial x}\right)$ divides equation (3.45) by dx.

$$\frac{\partial T_I}{\partial x} = \left(\frac{\partial T_I}{\partial \xi}\right)_{\zeta}\frac{\partial \xi}{\partial x} + \left(\frac{\partial T_I}{\partial \zeta}\right)_{\xi}\frac{\partial \zeta}{\partial x} \tag{3.48}$$

∂ζ/ ∂x=0. By using equation (3.39) into equation (3.48) the following expressions are obtained in the (ζ,ξ) coordinate system.

$$\frac{\partial T_I}{\partial x} = \frac{\partial T_I}{\partial \xi}\frac{\partial \xi}{\partial x} = \frac{1}{X(\zeta)}\frac{\partial T_I}{\partial \xi} \tag{3.49}$$

$$\frac{\partial^2 T_I}{\partial x^2} = \frac{\partial}{\partial x}\left(\frac{\partial T_I}{\partial \xi}\frac{\partial \xi}{\partial x}\right) = \frac{\partial}{\partial \xi}\left(\frac{\partial T_I}{\partial \xi}\frac{\partial \xi}{\partial x}\right)\frac{\partial \xi}{\partial x} = \frac{\partial^2 T_I}{\partial \xi^2}\left(\frac{\partial \xi}{\partial x}\right)^2 + \frac{\partial T_I}{\partial \xi}\left(\frac{\partial^2 \xi}{\partial \xi \partial x}\right)\frac{\partial \xi}{\partial x} \tag{3.50}$$

Since $\frac{\partial^2 \xi}{\partial \xi \partial x} = 0.$

$$\frac{\partial^2 T_I}{\partial x^2} = \frac{\partial^2 T_I}{\partial \xi^2}\left(\frac{\partial \xi}{\partial x}\right)^2 = \left(\frac{1}{X(\zeta)}\right)^2\frac{\partial^2 T_I}{\partial \xi^2} \tag{3.51}$$

Temperature of the frozen region (T_{II}) is function of time and space:

$$T_{II} = T_{II}(\zeta, \theta) \Rightarrow dT_{II} = \left(\frac{\partial T_{II}}{\partial \theta}\right)_{\zeta} d\theta + \left(\frac{\partial T_{II}}{\partial \zeta}\right)_{\theta} d\zeta \tag{3.52}$$

Temperature of frozen region's time derivative is:

$$\frac{\partial T_{II}}{\partial t} = \left(\frac{\partial T_{II}}{\partial \theta}\right)_{\text{Ţ}} \frac{\partial \theta}{\partial t} + \left(\frac{\partial T_{II}}{\partial \text{Ţ}}\right)_{\theta} \frac{\partial \text{Ţ}}{\partial t} \tag{3.53}$$

∂Ţ/ ∂t=1. By using equation (3.42) into equation (3.53) the following expressions are obtained in the (Ţ,θ) coordinate system.

$$\frac{\partial T_{II}}{\partial t} = \left[\frac{\mathrm{L}(\theta - 1) + \mathrm{X}(\text{Ţ})(1 - \theta)}{[\mathrm{L} - \mathrm{X}(\text{Ţ})]^2}\right] \frac{\partial \mathrm{X}(\text{Ţ})}{\partial \mathrm{t}} \frac{\partial T_{II}}{\partial \theta} + \frac{\partial T_{II}}{\partial \text{Ţ}} \tag{3.54}$$

Temperature of frozen region's x derivative is in terms of new coordinate system:

$$\frac{\partial T_{II}}{\partial x} = \left(\frac{\partial T_{II}}{\partial \theta}\right)_{\text{Ţ}} \frac{\partial \theta}{\partial x} + \left(\frac{\partial T_{II}}{\partial \text{Ţ}}\right)_{\theta} \frac{\partial \text{Ţ}}{\partial x} \tag{3.55}$$

$$\begin{aligned} \frac{\partial^2 T_{II}}{\partial \mathrm{x}^2} &= \frac{\partial}{\partial \mathrm{x}}\left(\frac{\partial T_{II}}{\partial \theta}\frac{\partial \theta}{\partial x}\right) = \frac{\partial}{\partial \theta}\left(\frac{\partial T_{II}}{\partial \theta}\frac{\partial \theta}{\partial x}\right)\frac{\partial \theta}{\partial x} \\ &= \frac{\partial^2 T_{II}}{\partial \theta^2}\left(\frac{\partial \theta}{\partial x}\right)^2 + \frac{\partial T_{II}}{\partial \theta}\left(\frac{\partial^2 \theta}{\partial \theta \partial x}\right)\frac{\partial \theta}{\partial x} \end{aligned} \tag{3.56}$$

$\frac{\partial^2 \xi}{\partial \xi \partial x} = 0$ and $\frac{\partial \text{Ţ}}{\partial x} = 0$.

Combining equations (3.43), (3.55) and (3.56), then gives the first and second derivatives of T_{II} with respect to x:

$$\frac{\partial T_{II}}{\partial x} = \frac{1}{[\mathrm{L} - \mathrm{X(t)}]} \frac{\partial T_{II}}{\partial \theta} \tag{3.57}$$

$$\frac{\partial^2 T_{II}}{\partial \mathrm{x}^2} = \left(\frac{1}{[\mathrm{L} - \mathrm{X(t)}]}\right)^2 \frac{\partial^2 T_{II}}{\partial \theta^2} \tag{3.58}$$

The energy equation in the dried layer terms becomes as follows in the (Ţ,ξ) coordinate system:

$$\frac{\partial T_{\mathrm{I}}}{\partial \mathrm{T}} = \frac{\alpha_{\mathrm{Ie}}}{\mathrm{X}(\mathrm{T})^2}\frac{\partial^2 T_{\mathrm{I}}}{\partial \xi^2} + \frac{1}{\mathrm{X}(\mathrm{T})}\left[\xi\frac{\partial \mathrm{X}(\mathrm{T})}{\partial \mathrm{T}}\frac{\partial \mathrm{T_I}}{\partial \xi} - \frac{c_{\mathrm{pg}}}{\rho_{\mathrm{Ie}}c_{\mathrm{pIe}}}\frac{\partial(N_{\mathrm{t}}T_{\mathrm{I}})}{\partial \xi}\right] + \frac{\Delta H_{\mathrm{v}}\rho_{\mathrm{I}}}{\rho_{\mathrm{Ie}}c_{\mathrm{pIe}}}\left(\frac{\partial C_{\mathrm{sw}}}{\partial \mathrm{T}}\right) \tag{3.59}$$

The energy equation in the frozen layer terms becomes as follows in the (Ƭ,θ) coordinate system:

$$\frac{\partial T_{\mathrm{II}}}{\partial \mathrm{T}} = \frac{\alpha_{\mathrm{II}}}{[L - X(\mathrm{T})]^2}\frac{\partial^2 T_{II}}{\partial \theta^2} - \left[\frac{\mathrm{L}(\theta - 1) + \mathrm{X}(\mathrm{T})(1 - \theta)}{[\mathrm{L} - \mathrm{X}(\mathrm{T})]^2}\right]\frac{\partial \mathrm{X}(\mathrm{T})}{\partial \mathrm{T}}\frac{\partial T_{II}}{\partial \theta} \tag{3.60}$$

The water vapor and inert gas mass flux can be expressed in the new coordinate system as:

$$\begin{aligned}\mathrm{N_w} &= -\frac{M_{\mathrm{w}}}{\mathrm{R}T_{\mathrm{I}}}\frac{\partial \xi}{\partial x}\left(\mathrm{k}_1\frac{\partial P_{\mathrm{w}}}{\partial \xi} + \mathrm{k}_2 P_{\mathrm{w}}\left(\frac{\partial P_{\mathrm{w}}}{\partial \xi} + \frac{\partial P_{\mathrm{in}}}{\partial \xi}\right)\right)\\ &= -\frac{M_{\mathrm{w}}}{\mathrm{R}T_{\mathrm{I}}}\frac{1}{X(t)}\left(\mathrm{k}_1\frac{\partial P_{\mathrm{w}}}{\partial \xi} + \mathrm{k}_2 P_{\mathrm{w}}\left(\frac{\partial P_{\mathrm{w}}}{\partial \xi} + \frac{\partial P_{\mathrm{in}}}{\partial \xi}\right)\right)\end{aligned} \tag{3.61}$$

$$\mathrm{N_{in}} = -\frac{M_{\mathrm{in}}}{\mathrm{R}T_{\mathrm{I}}}\frac{1}{X(t)}\left(\mathrm{k}_3\frac{\partial P_{\mathrm{in}}}{\partial \xi} + \mathrm{k}_4 P_{\mathrm{in}}\left(\frac{\partial P_{\mathrm{w}}}{\partial \xi} + \frac{\partial P_{\mathrm{in}}}{\partial \xi}\right)\right) \tag{3.62}$$

One can take the partial derivative of the mass flux with respect to x and their transformations to the new coordinate system are as follows:

$$\frac{\partial \mathrm{N_w}}{\partial \mathrm{x}} = -\frac{M_{\mathrm{w}}}{\mathrm{R}T_{\mathrm{I}}}\left[\mathrm{k}_1\frac{\partial^2 P_{\mathrm{w}}}{\partial x^2} + \mathrm{k}_2\frac{\partial P_{\mathrm{w}}}{\partial \mathrm{x}}\left(\frac{\partial P_{\mathrm{w}}}{\partial \mathrm{x}} + \frac{\partial P_{\mathrm{in}}}{\partial \mathrm{x}}\right) + \mathrm{k}_2 P_{\mathrm{w}}\left(\frac{\partial^2 P_{\mathrm{w}}}{\partial x^2} + \frac{\partial^2 P_{\mathrm{in}}}{\partial x^2}\right)\right] \tag{3.63}$$

$$\frac{\partial \mathrm{N_{in}}}{\partial \mathrm{x}} = -\frac{M_{\mathrm{in}}}{\mathrm{R}T_{\mathrm{I}}}\left[\mathrm{k}_3\frac{\partial^2 P_{\mathrm{in}}}{\partial x^2} + \mathrm{k}_4\frac{\partial P_{\mathrm{in}}}{\partial \mathrm{x}}\left(\frac{\partial P_{\mathrm{w}}}{\partial \mathrm{x}} + \frac{\partial P_{\mathrm{in}}}{\partial \mathrm{x}}\right) + \mathrm{k}_4 P_{\mathrm{in}}\left(\frac{\partial^2 P_{\mathrm{w}}}{\partial x^2} + \frac{\partial^2 P_{\mathrm{in}}}{\partial x^2}\right)\right] \tag{3.64}$$

$$\frac{\partial \mathrm{N_w}}{\partial \xi} = -\frac{M_\mathrm{w}}{\mathrm{R}T_\mathrm{I}}\left[\frac{1}{X(t)}\right]^2\left[\mathrm{k}_1\frac{\partial^2 P_\mathrm{w}}{\partial \xi^2} + \mathrm{k}_2\frac{\partial P_\mathrm{w}}{\partial \xi}\left(\frac{\partial P_\mathrm{w}}{\partial \xi} + \frac{\partial P_\mathrm{in}}{\partial \xi}\right) + \mathrm{k}_2 P_\mathrm{w}\left(\frac{\partial^2 P_\mathrm{w}}{\partial \xi^2} + \frac{\partial^2 P_\mathrm{in}}{\partial \xi^2}\right)\right] \tag{3.65}$$

$$\frac{\partial \mathrm{N_{in}}}{\partial \xi} = -\frac{M_\mathrm{in}}{\mathrm{R}T_\mathrm{I}}\left[\frac{1}{X(t)}\right]^2\left[\mathrm{k}_3\frac{\partial^2 P_\mathrm{in}}{\partial \xi^2} + \mathrm{k}_4\frac{\partial P_\mathrm{in}}{\partial \xi}\left(\frac{\partial P_\mathrm{w}}{\partial \xi} + \frac{\partial P_\mathrm{in}}{\partial \xi}\right) + \mathrm{k}_4 P_\mathrm{in}\left(\frac{\partial^2 P_\mathrm{w}}{\partial \xi^2} + \frac{\partial^2 P_\mathrm{in}}{\partial \xi^2}\right)\right] \tag{3.66}$$

The continuity equations for water vapor and inerts in the dried layer can be expressed in the new coordinate system as:

$$\frac{\partial \mathrm{P_w}}{\partial \mathrm{T}} = \frac{\xi}{X(t)}\frac{\partial \mathrm{X(T)}}{\partial \mathrm{T}}\frac{\partial \mathrm{P_w}}{\partial \xi} - \frac{\mathrm{R}T_\mathrm{I}}{\varepsilon M_\mathrm{w}}\left[\frac{1}{X(t)}\frac{\partial \mathrm{N_w}}{\partial \xi} + \rho_I\frac{\partial \mathrm{C_{sw}}}{\partial \mathrm{T}}\right] \tag{3.67}$$

$$\frac{\partial \mathrm{P_{in}}}{\partial \mathrm{T}} = \frac{\xi}{X(t)}\frac{\partial \mathrm{X(T)}}{\partial \mathrm{T}}\frac{\partial \mathrm{P_{in}}}{\partial \xi} - \frac{\mathrm{R}T_\mathrm{I}}{\varepsilon M_\mathrm{in}}\left[\frac{1}{X(t)}\frac{\partial \mathrm{N_{in}}}{\partial \xi}\right] \tag{3.68}$$

The desorption rate of bound water in the dried layer becomes:

$$\frac{\partial \mathrm{C_{sw}}}{\partial \mathrm{T}} = \frac{\xi}{X(t)}\frac{\partial \mathrm{X(T)}}{\partial \mathrm{T}}\frac{\partial \mathrm{C_{sw}}}{\partial \xi} - k_d C_{sw} \tag{3.69}$$

In the immobilizing coordinate system, the material balance equation at the interface becomes:

$$\mathrm{V} = \frac{\mathrm{dX(T)}}{\mathrm{dT}} = -\frac{\mathrm{N_w}\,|_{\xi=1}}{\rho_\mathrm{II} - \rho_\mathrm{Ie}} \tag{3.70}$$

The initial conditions in the new coordinate system are:

$$\mathrm{T_I} = \mathrm{T_{II}} = \mathrm{T_X} = T^0; \qquad 0 \le \xi \le 1; \quad \mathrm{T} = 0 \tag{3.71}$$

$$q_I = -k_{Ie}\frac{\xi}{X(\tau)}\frac{\partial T_I}{\partial \xi}\,|_{\xi=0}; \qquad \xi = 0; \quad \tau > 0 \tag{3.72}$$

$$q_I = \sigma F\left(T_{up}^4 - (T_I\,|_{\xi=0})^4\right); \qquad \tau > 0 \tag{3.73}$$

Energy balance at the moving interface becomes:

$$\frac{k_{II}}{[L - X(\tau)]}\frac{\partial T_{II}}{\partial \theta} - \frac{k_{Ie}}{X(\tau)}\frac{\partial T_I}{\partial \xi} + \frac{dX(\tau)}{d\tau}\left(\rho_{II}C_{pII}T_{II} - \rho_I C_{pI}T_I\right) + N_t C_{pg}T_x = -\Delta H_s N_t; \qquad \xi = 1; \quad \theta = 0, \quad \tau > 0 \tag{3.74}$$

$$T_I = T_x = T_{II}; \qquad \xi = 1; \quad \theta = 0, \quad \tau > 0 \tag{3.75}$$

The boundary condition for T_{II} becomes:

$$q_{II} = \frac{k_{II}}{[L - X(\tau)]}\frac{\partial T_{II}}{\partial \theta}\,|_{\theta=1}; \qquad \theta = 1, \quad \tau > 0 \tag{3.76}$$

$$q_{II} = k_f(T_{LP} - T_{II}\,|_{\theta=1}); \qquad \theta = 1, \quad \tau > 0 \tag{3.77}$$

The initial and boundary conditions for partial pressure of water vapor and inerts become:

$$P_w\,|_{\xi=0} = P_w^\circ, \quad P_{in|_{\xi=0}} = P_{in}^\circ; \qquad \xi = 0, \quad \tau = 0 \tag{3.78}$$

$$P_w\,|_{\xi=1} = f\left(T_I\,|_{\xi=1}\right); \qquad \xi = 1,, \quad \tau > 0 \tag{3.79}$$

$$\frac{1}{X(\tau)}\frac{\partial P_{in}}{\partial \xi}\,|_{\xi=1} = 0; \qquad \xi = 1, \quad \tau > 0 \tag{3.80}$$

There is no frozen layer and moving interface during the secondary drying stage. The equations in the dried layer can be transformed from the (t, x) coordinate system to the (ϒ,ξ) coordinate system by using the following equation:

$$\Upsilon = t \tag{3.81}$$

$$\xi = \frac{x}{L}, \quad 0 \le x \le L \tag{3.82}$$

With the coordinate system selected, we have:

$$\frac{\partial \Upsilon}{\partial \mathrm{x}} = 0, \quad \frac{\partial \Upsilon}{\partial \mathrm{t}} = 1 \tag{3.83}$$

$$\frac{\partial \xi}{\partial \mathrm{x}} = \frac{1}{\mathrm{L}}, \quad \frac{\partial^2 \xi}{\partial \mathrm{x}^2} = 0, \quad \frac{\partial \xi}{\partial \mathrm{t}} = 0 \tag{3.84}$$

The energy balance equation in the new coordinate system is:

$$\frac{\partial T_{\mathrm{I}}}{\partial \Upsilon} = \frac{\alpha_{\mathrm{Ie}}}{\mathrm{L}^2}\frac{\partial^2 T_{\mathrm{I}}}{\partial \xi^2} - \frac{c_{\mathrm{pg}}}{\rho_{\mathrm{Ie}} c_{\mathrm{pIe}}}\frac{1}{\mathrm{L}}\frac{\partial (N_{\mathrm{t}} T_{\mathrm{I}})}{\partial \xi} - \frac{\Delta H_{\mathrm{v}} \rho_{\mathrm{I}}}{\rho_{\mathrm{Ie}} c_{\mathrm{pIe}}}\left(\frac{\partial C_{\mathrm{sw}}}{\partial \Upsilon}\right); \quad 0 \le \xi \le 1, \quad \Upsilon > \Upsilon\,|_{x=L} \tag{3.85}$$

The initial and boundary conditions of energy balance equation for the secondary drying stage in the (ϒ,ξ) coordinate system are:

$$\mathrm{T_I} = \gamma(\xi); \qquad 0 \le \xi \le 1, \quad \Upsilon = \Upsilon\,|_{x=L} \tag{3.86}$$

$$\mathrm{q}_{\mathrm{I}|_{\xi=0}} = \frac{-k_{\mathrm{Ie}}}{\mathrm{L}}\frac{\partial T_{\mathrm{I}}}{\partial \xi}\,|_{\xi=0}; \qquad \xi = 0, \quad \Upsilon > \Upsilon\,|_{x=L} \tag{3.87}$$

$$\mathrm{q_I} = \sigma \mathrm{F}\left(T_{UP}^4 - T_I^4\,|_{\xi=0}\right); \qquad \xi = 0, \quad \Upsilon > \Upsilon\,|_{x=L} \tag{3.88}$$

$$q_{II} = \frac{-k_{Ie}}{L}\frac{\partial T_I}{\partial \xi}\,|_{\xi=1}; \qquad \xi = 1, \quad \tau > \tau\,|_{x=L} \tag{3.89}$$

$$q_{II} = \sigma F\left(T_{LP}^4 - T_I^4\,|_{\xi=1}\right); \qquad \xi = 1, \quad \tau > \tau\,|_{x=L} \tag{3.90}$$

$$q_{II} = k_f\left(T_{LP} - T_{II}\,|_{\xi=1}\right); \qquad \xi = 1, \quad \tau > \tau\,|_{x=L} \tag{3.91}$$

During secondary drying stage the dusty- gas model equations for water vapor and inerts become as follows:

$$N_W = -\frac{M_w}{RT_I}\frac{1}{L}\left(k_1\frac{\partial P_w}{\partial \xi} + k_2 P_w\left(\frac{\partial P_w}{\partial \xi} + \frac{\partial P_{in}}{\partial \xi}\right)\right) \tag{3.92}$$

$$N_{in} = -\frac{M_w}{RT_I}\frac{1}{L}\left(k_3\frac{\partial P_{in}}{\partial \xi} + k_4 P_{in}\left(\frac{\partial P_w}{\partial \xi} + \frac{\partial P_{in}}{\partial \xi}\right)\right) \tag{3.93}$$

In the new coordinate system the continuity equations for water vapor and inerts for the secondary drying stage become:

$$\frac{\partial P_w}{\partial \tau} = -\frac{RT_I}{\varepsilon M_w}\left[\frac{1}{L}\frac{\partial N_w}{\partial \xi} + \rho_I\frac{\partial C_{sw}}{\partial \tau}\right]; \qquad 0 \le \xi \le 1, \quad \tau > \tau\,|_{x=L} \tag{3.94}$$

$$\frac{\partial P_{in}}{\partial \tau} = -\frac{RT_I}{\varepsilon M_{in}}\frac{1}{L}\frac{\partial N_{in}}{\partial \xi}; \qquad 0 \le \xi \le 1, \quad \tau > \tau\,|_{x=L} \tag{3.95}$$

$$\frac{\partial C_{sw}}{\partial \tau} = -k_d C_{sw}; \qquad 0 \le \xi \le 1\,, \quad \tau > \tau\,|_{x=L} \tag{3.96}$$

The partial pressure initial and boundary conditions for the secondary drying stage are:

$$P_w = \delta(\xi); \qquad 0 \le \xi \le 1, \quad \tau = \tau\,|_{x=L} \tag{3.97}$$

$$P_{in} = \theta(\xi); \qquad 0 \le \xi \le 1, \quad \tau = \tau\,|_{x=L} \tag{3.98}$$

$$C_{sw} = v(\xi); \qquad 0 \le \xi \le 1, \quad \tau = \tau\,|_{x=L} \tag{3.99}$$

$$P_w = P_{w0}(\xi), \quad P_{in} = P_{in0}(\xi); \qquad \xi = 0, \quad \tau > \tau\,|_{x=L} \tag{3.100}$$

$$\frac{\partial P_w}{\partial \xi}\,|_{\xi=1} = 0; \qquad \xi = 1, \quad \tau > \tau\,|_{x=L} \tag{3.101}$$

$$\frac{\partial P_{in}}{\partial \xi}\,|_{\xi=1} = 0; \qquad \xi = 1, \quad \tau > \tau\,|_{x=L} \tag{3.102}$$

3.5. Numerical Analysis of Mathematical Model

The method of weighted residuals is a general method for the solution of differential equations which reduce the number of independent variables or the problem domain dimension. The basic idea of the method is to approximate the solution of the problem over a domain by a function form called trial function. The trial function's form is specified but it has adjustable constants. The trial function is chosen so as to give a good solution to the original differential equation. The Orthogonal Collocation method is one of several weighted residual method where polynomial approximate solution is substituted into the differential equation to form the residual [Ramirez, 1997].

The model equations were solved by using the orthogonal collocation based on polynomial approximation-Jacobi method in this context. The dynamic model was constructed in MATLAB R2011b (7.13.0.564) software package. Jacobi polynomial of order 10 is used for freeze-drying process modeling. Complete MATLAB coding for mathematical modeling of turkey meat are attached in Appendix B. In order to obtain the locations of the collocation points and derivatives and integral weighting matrices and vectors, the colloc m-file was used based on the methods described by [Villadsen and Michelsen, 1978]. To define the matrices A_{ij} and B_{ij}, we evaluate this expression at the selected collocation points; we also differentiate it and evaluate the

result at the collocation points. This method transforms the partial differential equations to a set of ordinary differential equations.

3.5.1. Collocation Method

The Orthogonal Collocation method is used to obtain approximate solutions to differential equations in the model. Let us consider the boundary value problem involving the second order differential equation. Suppose that the range of x is $0 \leq x \leq 1$. The boundary conditions are $y(0) = 0$ and $y(1) = 1$.

$$y'' = f(x, y, y') \tag{3.103}$$

If we have an nth order polynomial, P_n(x), which provide a good approximation to the solution, then we can write,

$$P_n(x) \approx y(x) \tag{3.104}$$

$$P_n(x) = C_0 + C_1 x + C_2 x^2 + \cdots . . + C_n x^n \tag{3.105}$$

P_n(x) is known as trial function. The difference

$$R(x) = \frac{d^2 P_n(x)}{dx^2} - F\left[x, P_n(x), \frac{dP_n(x)}{dx}\right] \tag{3.106}$$

is called the residual. Our objective is to choose the coefficients of the polynomial so that the residual is the smallest. This is achieved by the following condition:

$$\int_0^1 W_j R(x) dx = 0 \tag{3.107}$$

where W_j are called weight functions. This method is also known as the method of weighted residuals. The weight functions in the collocation method are Dirac delta functions $W_j = \delta(x - x_j)$. From its fundamental property, equation (3.107) becomes

$$\int_0^1 W_j R(x)dx = R(x_j) = 0 \tag{3.108}$$

The coefficients $C_i\ (i = 0, 1, \dots, m)$ are chosen such that at certain points, $(x_{j,}\ j = 0, 1, \dots, n)$, called collocation points, $R(x)|_{x=x_j}$ in equation (3.106) becomes zero. The collocation points need not be equispaced. They can be unequally spaced as well. The collocation methods are most efficient when the internal points are chosen as zeros of orthogonal polynomials. In that case, the method is called orthogonal collocation [Ghosh, 2006]. The basic property of any orthogonal polynomial is:

$$\int_a^b w(x)P_n\,(x)P_m(x)dx = \begin{cases} 0 & n \neq m \\ h_n > 0 & n = m \end{cases} \tag{3.109}$$

Here, the polynomial $P_n\,(x)$ is orthogonal over the domain $[a, b]$ [Ramirez, 1997]. Some of the well known orthogonal polynomials are Jacobi, Legendre, Chebyshev, Laguerre and Hermite polynomials. The trial function is a linear combination of the polynomials $P_n\,(x)$. The number of internal collocation points is (n-2). Apart from these, there are two boundary values. 1 is the first collocation point (x=0) and n+2 is the last collocation point (x=1). For the collocation method, we will force the differential equation to be satisfied at the collocation points. In order to so, we need to evaluate the function and its derivatives at the collocation points.

$$\mathrm{y(x)} = b + cx + x(1 - x)\sum_{i=2}^{n+1} \mathrm{a_i\ P_{i-1}\,(x)} = \sum_{i=1}^{n+2} \mathrm{d_i\ P_{i-1}\,(x)} \tag{3.110}$$

At a collocation point x_j we have:

$$y(x_j) = \sum_{i=1}^{n+2} \mathrm{d_i}\ \mathrm{x_j}^{(\mathrm{i}-1)},\ j = 1, 2, \ldots, n{+}2 \tag{3.111}$$

We can write equation (3.110) in matrix form as:

$$\begin{bmatrix} y(1) \\ y(2) \\ \vdots \\ y(n+2) \end{bmatrix} = \begin{bmatrix} 1 & x_1 & {x_1}^2 & \ldots & {x_1}^{n+1} \\ 1 & x_2 & {x_2}^2 & \ldots & {x_2}^{n+1} \\ \vdots & \vdots & \vdots & \vdots & \vdots \\ \vdots & \vdots & \vdots & \vdots & \vdots \\ 1 & x_{n+2} & {x_{n+2}}^2 & \ldots & {x_{n+2}}^{n+1} \end{bmatrix} \begin{bmatrix} d1 \\ d2 \\ \vdots \\ dn+2 \end{bmatrix} \tag{3.112}$$

The set of collocation points (n) and the boundary points can be expressed in terms of an unknown vector of coefficients d as:

$$y = Q\ d \tag{3.113}$$

where Q is a known matrix and is given in terms of the known collocation point x_j raised to an appropriate collocation order, i,

$$Q_{ij} = {x_j}^{i-1} \tag{3.114}$$

The vector y and d are of order (n+2) and the matrix Q of order (n+2, n+2). The first and second derivative of the trial function at a collocation point is given by

$$\frac{\mathrm{dy_j}}{\mathrm{dx}} = \sum_{i=1}^{n+2} (\mathrm{i}-1)\ \mathrm{x_j}^{(\mathrm{i}-2)} \mathrm{d_i} \tag{3.115}$$

$$\frac{\mathrm{d^2y_j}}{\mathrm{dx^2}} = \sum_{i=1}^{n+2} (\mathrm{i}-1)(\mathrm{i}-2)\ \mathrm{x_j}^{(\mathrm{i}-3)} \mathrm{d_i} \tag{3.116}$$

Put these formulas in matrix notation, where Q, C, D, A and B are n+2 by n+2 matrices. The set of relations of equations (3.115) and (3.116) at the collocation and boundary points can be expressed as

$$\frac{dy}{dx} = C\,d = C\,Q^{-1}y = A\,y \tag{3.117}$$

$$\frac{d^2y}{dx^2} = D\,d = D\,Q^{-1}y = B\,y \tag{3.118}$$

where $C_{ij} = (i-1)\,x_j^{(i-2)}$ and $D_{ij} = (i-1)(i-2)\,x_j^{(i-3)}$ [Ramirez, 1997].

The original interval for the Legendre polynomial is $[-1,1]$, but since we are considering x in the interval $0 \le x \le 1$, we can transform the Legendre polynomials using the transformation $z = (x+1)/2$. The first four Legendre polynomials and their transformed counterparts are given in Table 3.1 [Ghosh, 2006].

Table 3.1: First Four Legendre Polynomials.

n	**Legendre Polynomial**	**Original** $[-1, 1]$	**Transformed** $[0, 1]$
0	$P_0(x)$	1	1
1	$P_1(x)$	x	$2x-1$
2	$P_2(x)$	$\frac{3x^2-1}{2}$	$6x^2-6x+1$
3	$P_3(x)$	$\frac{5x^3-3x}{2}$	$20x^3-30x^2+12x-1$
4	$P_4(x)$	$\frac{35x^4-30x^2+3}{8}$	$70x^4-140x^3+90x^2-20x+1$

The roots x_i for the shifted Legendre polynomials are given in Table 3.2 and they specify the collocation points to be used in the method of weighted residuals [Ramirez, 1997].

Table 3.2: Roots for Shifted Legendre Polynomials.

n	Legendre Polynomial
1	0.5
2	0.2113 0.7887
3	0.1127 0.5000 0.8873
4	0.0694 0.3300 0.6700 0.9306

For example, the elements of matrices A and B for n=2. The roots are $x_1 = 0,\ x_2 = 0.2113,\ x_3 = 0.7887,\ x_4 = 1.$

The Q, C and D matrices have constant values derived from the roots. These three matrices are generated below:

$$Q = \begin{bmatrix} 1 & x_1 & {x_1}^2 & {x_1}^3 \\ 1 & x_2 & {x_2}^2 & {x_2}^3 \\ 1 & x_3 & {x_3}^2 & {x_3}^3 \\ 1 & x_4 & {x_4}^2 & {x_4}^3 \end{bmatrix} = \begin{bmatrix} 1 & 0 & 0 & 0 \\ 1 & 0.2113 & 0.04466 & 0.0094367 \\ 1 & 0.7887 & 0.62202 & 0.49057 \\ 1 & 1 & 1 & 1 \end{bmatrix} \tag{3.119}$$

$$C = \begin{bmatrix} 0 & 1 & 2x_1 & 3{x_1}^2 \\ 0 & 1 & 2x_2 & 3{x_2}^2 \\ 0 & 1 & 2x_3 & 3{x_3}^2 \\ 0 & 1 & 2x_4 & 3{x_4}^2 \end{bmatrix} = \begin{bmatrix} 0 & 1 & 0 & 0 \\ 0 & 1 & 0.42264 & 0.13397 \\ 0 & 1 & 1.57736 & 1.86605 \\ 0 & 1 & 2 & 3 \end{bmatrix} \tag{3.120}$$

$$D = \begin{bmatrix} 0 & 0 & 2 & 6x_1 \\ 0 & 0 & 2 & 6x_2 \\ 0 & 0 & 2 & 6x_3 \\ 0 & 0 & 2 & 6x_4 \end{bmatrix} = \begin{bmatrix} 0 & 0 & 2 & 0 \\ 0 & 0 & 2 & 1.26762 \\ 0 & 0 & 2 & 4.73208 \\ 0 & 0 & 2 & 0 \end{bmatrix} \tag{3.121}$$

The inverse of Q matrix is computed as:

$$Q^{-1} = \begin{bmatrix} 1 & 0 & 0 & 0 \\ -7.0004 & 8.1966 & -2.1964 & 1.0001 \\ 12.0004 & -18.5887 & 12.5887 & -6.0001 \\ -6 & 10.3921 & -10.39 & 6 \end{bmatrix} \tag{3.122}$$

Thus, the discretization matrices A and B for n= 2 are given by:

$$A = \underbrace{\begin{bmatrix} 0 & 1 & 0 & 0 \\ 0 & 1 & 0.42264 & 0.13397 \\ 0 & 1 & 1.57736 & 1.86605 \\ 0 & 1 & 2 & 6 \end{bmatrix}}_{C} x \underbrace{\begin{bmatrix} 1 & 0 & 0 & 0 \\ -7.0004 & 8.1966 & -2.1964 & 1.0001 \\ 12.0004 & -18.5887 & 12.5887 & -6.0001 \\ -6 & 10.3921 & -10.392 & 6 \end{bmatrix}}_{Q^{-1}} \tag{3.123}$$

$$A = \begin{bmatrix} -7.0004 & 8.1966 & -2.1964 & 1.0001 \\ -2.7324 & 1.7325 & 1.7318 & -0.7320 \\ 0.7323 & -1.7323 & -1.7320 & 2.7321 \\ -0.9996 & 2.1955 & -8.1957 & 6.9999 \end{bmatrix} \tag{3.124}$$

$$B = \underbrace{\begin{bmatrix} 0 & 0 & 2 & 0 \\ 0 & 0 & 2 & 1.26762 \\ 0 & 0 & 2 & 4.73208 \\ 0 & 0 & 2 & 6 \end{bmatrix}}_{D} x \underbrace{\begin{bmatrix} 1 & 0 & 0 & 0 \\ -7.0004 & 8.1966 & -2.1964 & 1.0001 \\ 12.0004 & -18.5887 & 12.5887 & -6.0001 \\ -6 & 10.3921 & -10.392 & 6 \end{bmatrix}}_{Q^{-1}} \tag{3.125}$$

$$B = \begin{bmatrix} 24.0008 & -37.1774 & 25.1770 & -12.0002 \\ 16.3933 & -24.0010 & 12.0006 & -4.3927 \\ -4.3917 & 11.9988 & -23.9992 & 16.3923 \\ -11.9992 & 25.1752 & -37.1756 & 23.9998 \end{bmatrix} \tag{3.126}$$

The collocation method applied to the boundary value problem (3.103) and gives the following equation:

$$\sum_{i=1}^{n+2} \mathrm{B_{ij}\, y_j} = \mathrm{f}\left(\mathrm{x_j}, \mathrm{y_j} \sum_{j=1}^{n+2} \mathrm{A_{ij}\, y_j} \right) \tag{3.127}$$

The method converts the partial differential equations into ordinary differential equations with the discretization matrices A and B. Differential equation can be expressed using A and B matrices as follows:

$$\frac{dy_j}{dx} = \sum_{j=1}^{n+2} A_{i,j}\, d_i \tag{3.128}$$

$$\frac{d^2y_j}{dx^2} = \sum_{j=1}^{n+2} B_{i,j}\, d_i \tag{3.129}$$

The partial differential equations are transformed to the ordinary differential equations with matrices A_{ij} and B_{ij}. For example, the energy equation (3.2) and boundary condition equations (3.5) and (3.6) at $x = 0$ in dried layer is as follows:

$$\frac{\partial T_I}{\partial t} = \alpha_{Ie}[B][T_I] - \frac{c_{pg}}{\rho_{Ie} c_{pIe}}[N_t][A][T_I] + \frac{\Delta H_v \rho_I}{\rho_{Ie} c_{pIe}} \left(\frac{\partial C_{sw}}{\partial t}\right) \tag{3.130}$$

$$q_I = -k_{Ie} \sum_{j=1}^{n} A\,(1,j)\; T_I\,(j) = \sigma F\left(T_{up}^4 - (T_I\,|_{x=0})^4\right) \tag{3.131}$$

$$k_{Ie}\left(A(1,1)T\,|_{x=0} + A(1,2)T(2) + .. + A(1,n)T(n)\right) = \sigma F\left(T_{up}^4 - (T_I\,|_{x=0})^4\right) \tag{3.132}$$

$$T\,|_{x=0} = \frac{-k_{Ie} \sum_{j=2}^{n} A\,(1,j)\; T_I\,(j) - \sigma F\left(T_{up}^4 - (T_I\,|_{x=0})^4\right)}{k_{Ie}\, A(1,1)} \tag{3.133}$$

3.6. Parameter Estimation

The parameter estimation was carried out using Lsqcurvefit function from the optimization toolbox of MATLAB R2011b (7.13.0.564) software package. The function Lsqcurvefit allowed solving nonlinear data fitting equations using the least square method with the implementation of the Levenberg-Marquardt method. An iterative computation procedure for estimating the parameters is used. For each iteration, if the difference between experimental data and theoretical data that obtained by solving dynamic mathematical model is high, the initial guess of parameters was altered until the difference is minimum. This procedure is identical to

the nonlinear least-square method where the sum of square of error (SSE) between experimental data and theoretical data minimized to obtain the best fitted parameters of the model [Kuu et al., 1995].

$$SSE = \sum_{i=1}^{N} (m_{exp} - m_t)^2 \tag{3.134}$$

where m_{exp} and m_t are the experimental and theoretical data points respectively, N denotes number of the experimental data points. The entire computation scheme that uses Lsqcurvefit algorithm is given in Figure 3.6.

Lsqcurvefit algorithm requires the initial guesses and range for the parameters, the given input data (m_{exp}) and the observed output data (m_t) to perform parameter estimation. In this study, the given input data are the experimental amount of removed water that was measured every two hours starting from the beginning to end of freeze-drying process and the temperature data that was measured every half hour starting from the beginning to end of primary drying stage. The observed output data calculated for the same time span of the given input data, by solving dynamic mathematical model that presented in this study.

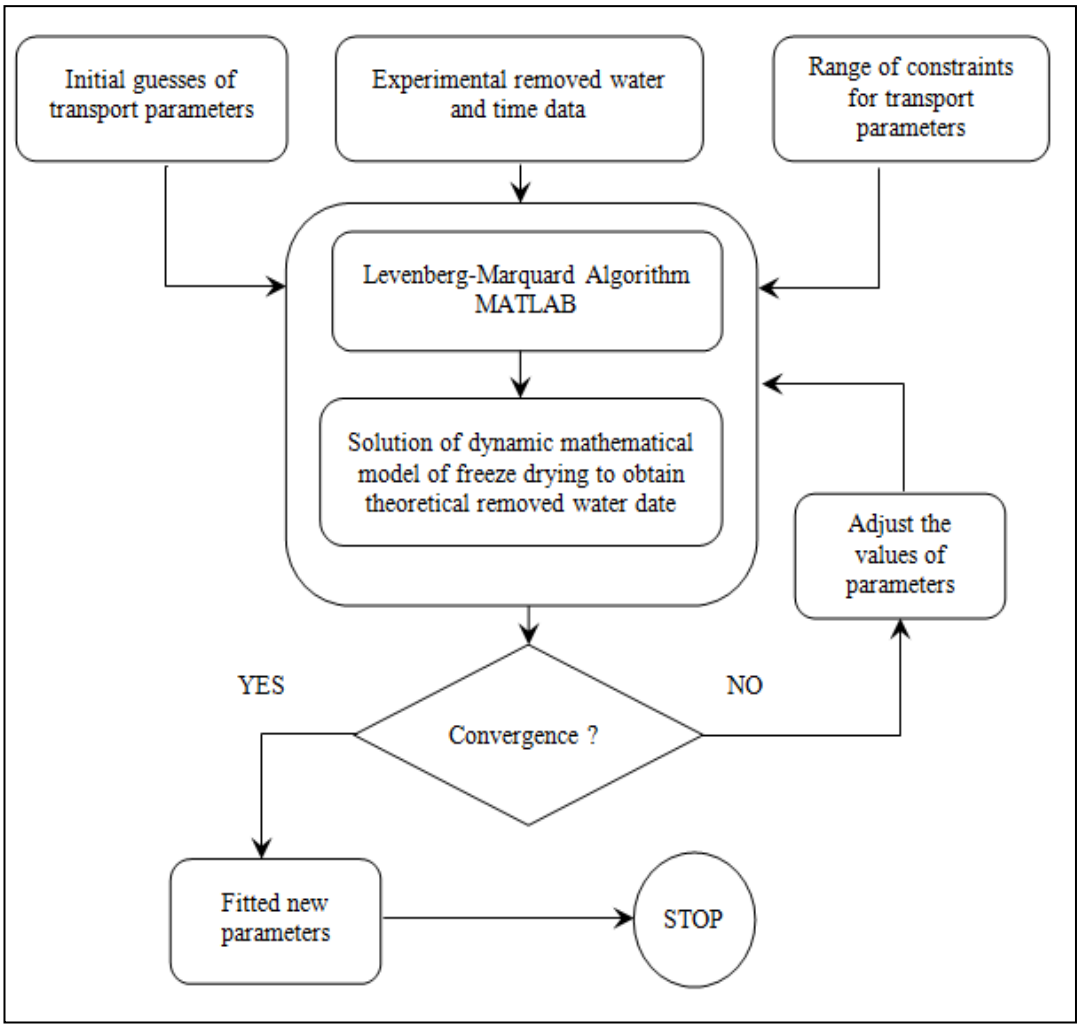

Figure 3.6: The entire computation scheme of the freeze-drying process.

4. RESULTS AND DISCUSSION

4.1. Experimental Freeze-Drying Results

The meat product experimental tray, surface and center point temperature profiles for 12.4 mm thick turkey meat slabs during drying stage of the freeze-drying process is shown in Figure 4.1. It can be seen that the experimental surface, T(t, x=0), and center point temperature, T(t, x=L/2), of the sample, initially increases quickly because of the higher initial temperature difference between the temperature of sample surface and heating plate and after the increment slows down in time because of the gradual decrease in temperature differences [Chakraborty et al., 2006].

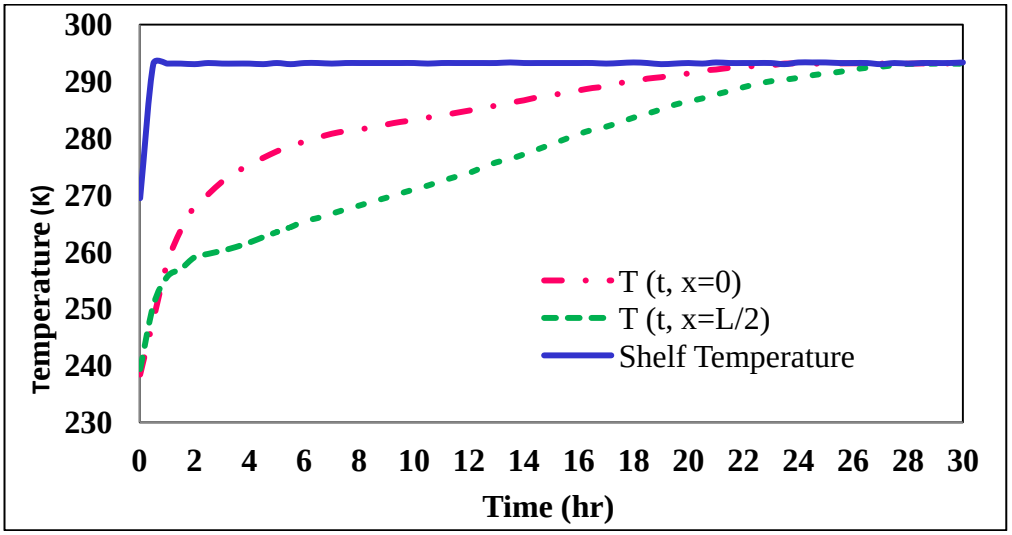

Figure 4.1: Profiles for the shelf and product temperature evaluation in time at positions x=0, x=L/2 during the duration of the freeze-drying stage for 12.4 mm thick turkey meat slab.

Amount of removed water and the residual water within the meat product during the freeze-drying process are presented in Table 4.1. The freeze-drying curve of turkey breast meat is shown in Figure 4.2 according to dimensionless moisture content ($WM(t)/WM_o$, Water Remaining/Initial Moisture Content, %). As matrix dries out, the kinetics slow down, primarily because sublimated vapor passes through a dry layer with increasing thickness over time and, at the end of the process, because water is progressively more bound as drying proceeds. When only

desorption of highly bound water takes place, freeze-drying kinetics are very slow [Ratti, 2012]. Water content of fresh turkey breast meat was % 74.838 wet bases. Figure4.3 shows the completely dried turkey meat by using freeze-dryer.

Table 4.1: Amount of Removed Water and Residual Water Content of Product.

Time (Hour)	**Amount of Removed Water for 12.4 mm thickness (g)**	**Residual Water for 12.4 mm thickness (%)**	**Amount of Removed Water for 14.5 mm thickness (g)**	**Residual Water for 14.5 mm thickness (%)**
0	0.000	100.00	0.000	100.00
2	6.180	76.99	7.258	76.79
4	11.435	57.42	13.458	56.97
6	15.518	42.20	17.614	43.70
8	18.995	29.25	20.820	33.45
10	21.671	19.28	23.270	25.63
12	23.925	10.88	25.454	18.64
14	24.981	6.95	27.157	13.20
16	25.552	4.83	28.540	8.78
18	26.037	3.02	29.431	5.93
20	26.334	1.91	30.108	3.76
22	26.508	1.26	30.568	2.29
24	26.599	0.92	30.848	1.40
26	26.650	0.73	30.982	0.97
28	26.681	0.62	31.026	0.83
30	-	-	31.080	0.65
32	-	-	31.102	0.59

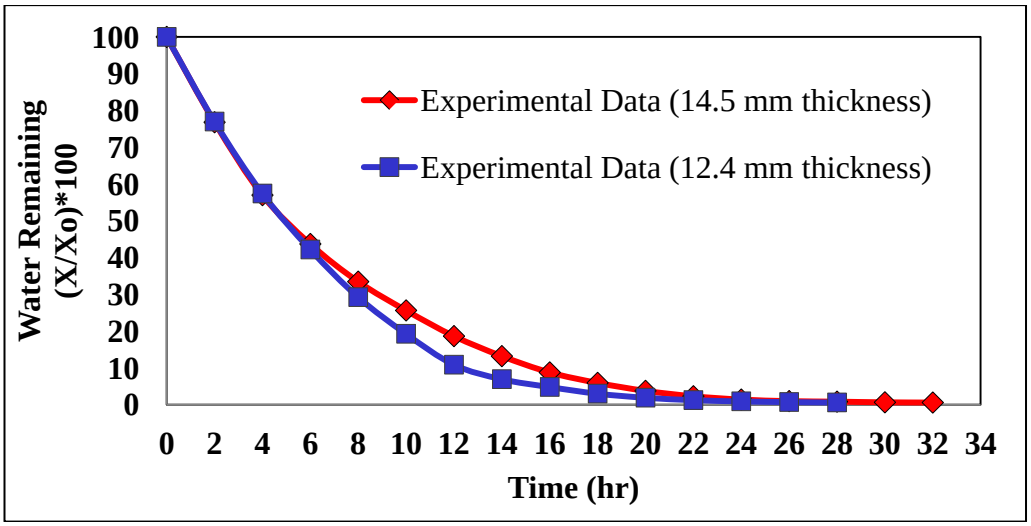

Figure 4.2: Change in water content with respect to drying time during the duration of freeze-drying of turkey breast meat sample for different sample thicknesses.

Figure 4.3: Turkey meat slabs completely dried.

4.2. Model Results and Discussion

The theoretical results for the freeze-drying of turkey meat were obtained by solving partial differential equations (3.2), (3.3), (3.12)-(3.14) and (3.22) along with initial and boundary condition that is given in equations (3.4)-(3.11) and equations (3.17)-(3.21) for the primary drying stage and equations (3.12)-(3.14) and (3.23) along with the initial and boundary condition that is given in equations (3.24)-(3.33) for the secondary drying stage simultaneously. Values of the parameters as well as the expressions employed in the evaluation of certain parameters used in the model are given in Table 4.2 and Table 4.3.

Table 4.2: Expressions and Values of the Physical and Transport Properties of Turkey Meat.

Symbol	Value or Expression	References
C_{0l}	$7.219x10^{-15}$ m^2	[Sadikoglu and Liapis, 1997]
C_2	0.19	[King, 1970]
C_{pg}	1.6166 kJ/kg K	[Sadikoglu and Liapis, 1997]
$C_{pıe}$	$C_{pıe}= (W_wC_{p,w}+W_pC_{p,p}+W_{fa}C_{p,fa}+W_aC_{p,a})$ kJ/kg K	[Ashrae, 2006].
	$C_{p,w}=4.1762-9,0862x10^{-5}T+5.4731x10^{-6}T^2$	
	$C_{p,p}=2.0082+1.2089x10^{-3}T-1.3129x10^{-6}T^2$	
	$C_{p,fa}=1.9842+1.4733x10^{-3}T-4.8008x10^{-6}T^2$	
	$C_{p,a}=1.0926+1.8896x10^{-3}T-3.6817x10^{-6}T^2$	
$C_{pıı}$	$C_{pıe}= (W_{ice}C_{p,i}+W_pC_{p,p}+W_{fa}C_{p,f\,a}+W_aC_{p,a})$ kJ/kg K	[Ashrae, 2006]
	$C_{p,w}= 2.0623+6.0769x10^{-3}T$	
	$C_{p,p}=2.0082+1.2089x10^{-3}T-1.3129x10^{-6}T^2$	
	$C_{p,fa}=1.9842+1.4733x10^{-3}T-4.8008x10^{-6}T^2$	
	$C_{p,a}=1.0926+1.8896x10^{-3}T-3.6817x10^{-6}T^2$	
$D^o_{w.in}$	$8.729x10^{-7}(T_I+T_x)^{2.334}$ N/s	[Litchfield and Liapis, 1982]
F	1	[Sadikoglu, 1998]
f (T_x)	$133.3224[\exp(-2445.5646/T_x +8.2312 \log_{10}(T_x)-$	[Sadikoglu and Liapis, 1997]
	$0.01677006T_x +1.20514\ x10^{-5}T_x\ ^2-6.757169)]$ N/m^2	
$k_{ıı}$	$(0.48819/T_{II})+0.4685x10^{-3}$ kW/m K	[Sadikoglu and Liapis, 1997]
k_d	$6.480x10^{-7}$ s^{-1} (during the primary drying stage)	[Sadikoglu and Liapis, 1997]
P_w^o	1.07 N/m^2	
P_o	11.07 N/m^2	
T^o	233.15 K	
T_m	263.84 K	[Litchfield and Liapis, 1982]
T_{scor}	333.15 K	[Litchfield and Liapis, 1982]
T_{LP}	293.15 K	
T_{UP}	293.15 K	
ΔH_s	2840 kJ/kg	[Sadikoglu and Liapis, 1997]
ΔH_v	2687.4 kJ/kg	[Sadikoglu and Liapis, 1997]
Ɛ	0.74	[Valdes-Fragaso et al., 2008]
μ_{mx}	$18.4858x10^{-7}[T_I^{1.5}/(T_I+650)]$ kg/m s	[Sadikoglu and Liapis, 1997]
$\rho_ı$	333 kg/m^3	[Litchfield and Liapis, 1982]
$\rho_{ıı}$	1133 kg/m^3	[Litchfield and Liapis, 1982]
σ	$5.676x10^{-11}$ $kW/m^2\ K^4$	[Sadikoglu and Liapis, 1997]

The parameters which are difficult to measure directly such as weight fraction of bound water, C^{o}_{sw}, thermal conductivity of dried layer, k_{Ie}, Knudsen diffusivity for water vapor, k_w, film thermal conductivity, k_f, and desorption rate constant of bound water for secondary drying stage, k_d, were estimated by matching experimental freeze-drying data with the predictions of the theoretical model, using Levenberg-Marquardt algorithm of MATLAB (based on non-linear least square method). The remaining parameters and expressions that characterize the heat and mass transfer mechanisms of the model are given in Table 4.3. The heat capacity of the turkey meat was calculated by using composition data (i.e., water, protein, ash and fat) in conjunction with temperature dependent mathematical models of heat capacity of the individual food constituents [Ashrae, 2006]. Turkey breast meat contains approximately 74.838% water, 19.809% protein [Yalçın, 2014] and 4.474% fat. C_{pIe} and C_{pII} were calculated as 2.5184 kJ/kg K and 1.9371 kJ/kg K, respectively. Bound water is a characteristic property of a food and that represents portion of water that is bound to the solids in the food and it remains unfrozen at the end of the freezing process. The amount of bound water varies significantly depending on protein content of the food. The value of bound water for meat and fish is equal approximately 0.4 g of bound water per g of dry protein [DeMan, 1999]. Initial value of bound water, C^{o}_{sw}, is calculated with regards to the procedure suggested in the literature. In this study, contribution of desorption of bound water to total mass flux of water removed during primary drying stage is considered.

Table 4.3: Estimated Model Parameters.

Parameter	**Initial Guesses for Parameters**	**Estimated Model Parameters**
C^{o}_{sw}(kgwater/kg solid)	0.3150	0.3276
k_d (s^{-1})	7.8×10^{-5}	5.07×10^{-5}
k_f (kW/m^2K)	$1.5358 \times 10^{-3}P$	$2.0580 \times 10^{-3}P$
k_{ie} (kW/m K)	$85x10^{-6}$ [1-0.325exp (- $5x10^{-3}$ P)]	$44.2x10^{-6}$ [1-0.325exp (- $5x10^{-3}$ P)]
K_w (m^2/s)	$1.6395x10^{-4}(T_I+T_x)^{0.5}$	$3.1151 \times 10^{-5}(T_I+T_x)^{0.5}$

Table 4.3 represents estimated model parameters as well as initial guesses for these parameters with the acceptable tolerance. The initial guesses for parameters of

thermal conductivity of dried layer, k_{le}, and Knudsen diffusivity for water vapor, k_w, data were used from modeling study of turkey breast meat where the heat flux was parallel to fiber direction [Litchfield and Liapis, 1982]. The initial guesses for thermal conductivity, k_f, and desorption rate constant of bound water for secondary drying stage, k_d, data for skim milk were used from [Sadikoglu and Liapis, 1997].

The values of the parameters that characterize thermal conductivity of dried layer, k_{le}, and Knudsen diffusivity, k_w, in the dried layer are 48% and 81%, respectively, less when they compared to the values of the parameters used in work of [Litchfield and Liapis, 1982]. This is because different freezing procedure and different freezing temperature used in this study when it was compare to work of [Litchfield and Liapis, 1982] to obtain frozen sample prior to freeze-drying. The size and the shape of the dendritic ice crystals formed upon freezing depend heavily on the freezing rate of the sample. In their work, [Litchfield and Liapis, 1982] used relatively higher freezing temperature of 241.8 K compare to freezing temperature of 233 K used in this work, causes lower freezing rate. Lower freezing rate means the larger dendritic ice crystals formed in sample during freezing that result in higher water vapor mass transfer rates in the pores of the dried product. Also, in their work, [Litchfield and Liapis, 1982] replace the turkey breast meat in the tray of the freeze-dryer where dendritic fiber direction was parallel to heat and mass flux direction while in this work dendritic fiber direction was perpendicular to heat and mass flux direction.

It can be seen in Figure 4.4, the partial pressure of water vapor at x=X for the meat product is plotted versus time during the primary drying stage. It can be observed that the value of pressure, $P_w(t,x=X)$, increases with time in order to overcome the increased mass transfer resistance due to the increasing with time size of dried layer [Liapis and Bruttini, 2009].

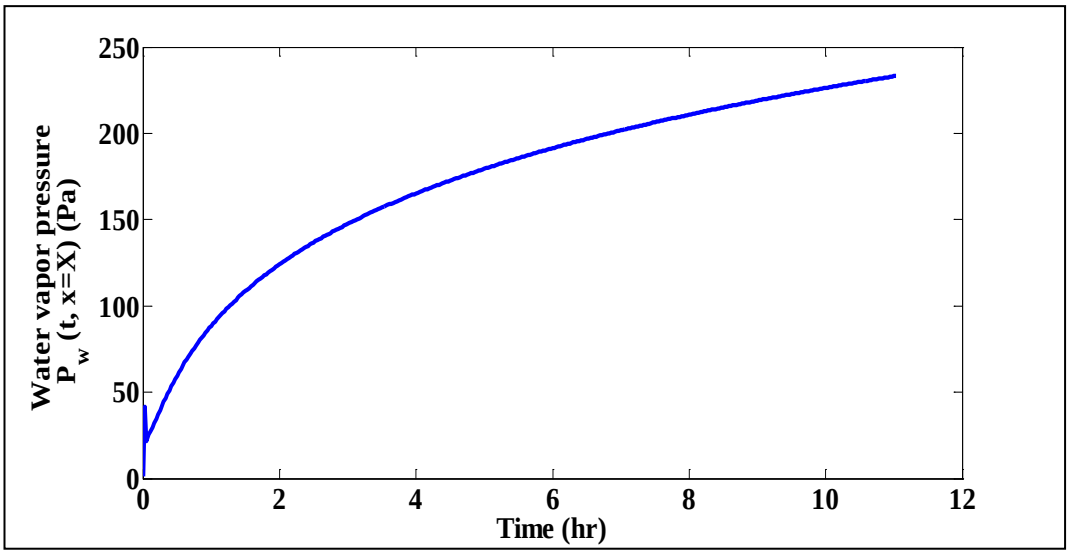

Figure 4.4: Water vapor pressure at position x=X for 12.4 mm thick turkey meat slab.

The meat product temperature profiles in dried and frozen regions are plotted versus time during primary drying stage of the freeze-drying process in Figure 4.5 and Figure 4.6. As expected the temperature in the dried region is higher than the temperature in the frozen region. Therefore the vapor from the sublimation interface is superheated, and no recondensation occurs in this region [Fey and Boles, 1988]. The temperature distribution within the frozen region (Figure 4.6) is smaller than dried region as a result of the much higher thermal conductivity of the frozen layer than the effective thermal conductivity of the dried layer. Particularly, at the beginning of the drying phase, the temperature exhibits a sharp reduction, and then a high increase of temperature followed by a softer evolution. Reduction of product temperature is due to the energy absorbed from the frozen mass for the sublimation [Velardi and Barresi, 2008]. Temperatures in the dried layer (Figure 4.5) decreases progressively from the top surface to the moving interface. The surface temperature is the highest while sublimation interface temperature is the lowest in the profile due to the consumption of energy for the sublimation of ice [Liapis and Bruttini, 2009]. The vacuum between the ice interface and the condenser ensures that the interface temperature is always very low [Mellor, 1978].

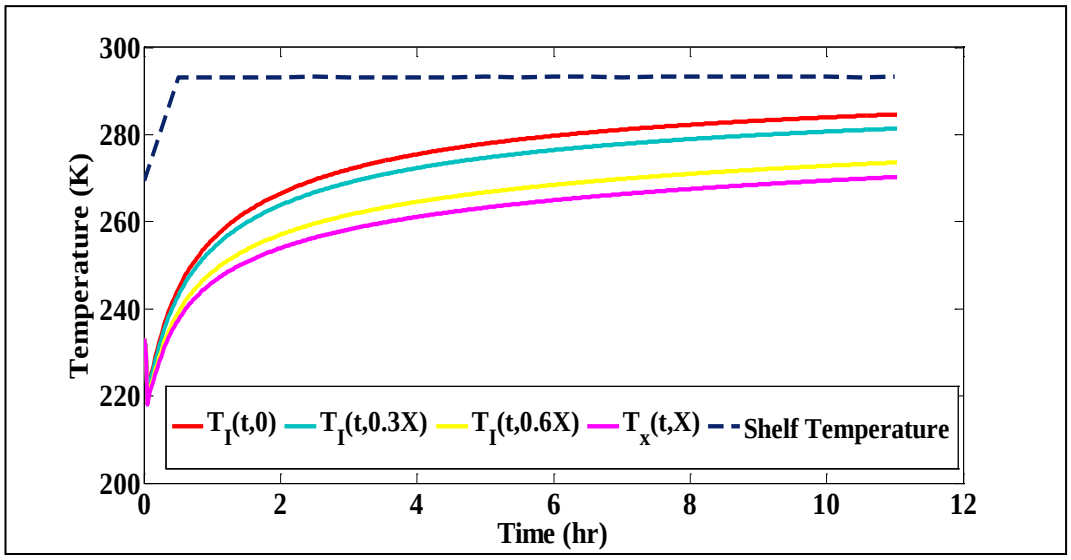

Figure 4.5: Profiles for the product temperature evaluation in time at different sample positions of dried layer for 12.4 mm thick turkey meat slab.

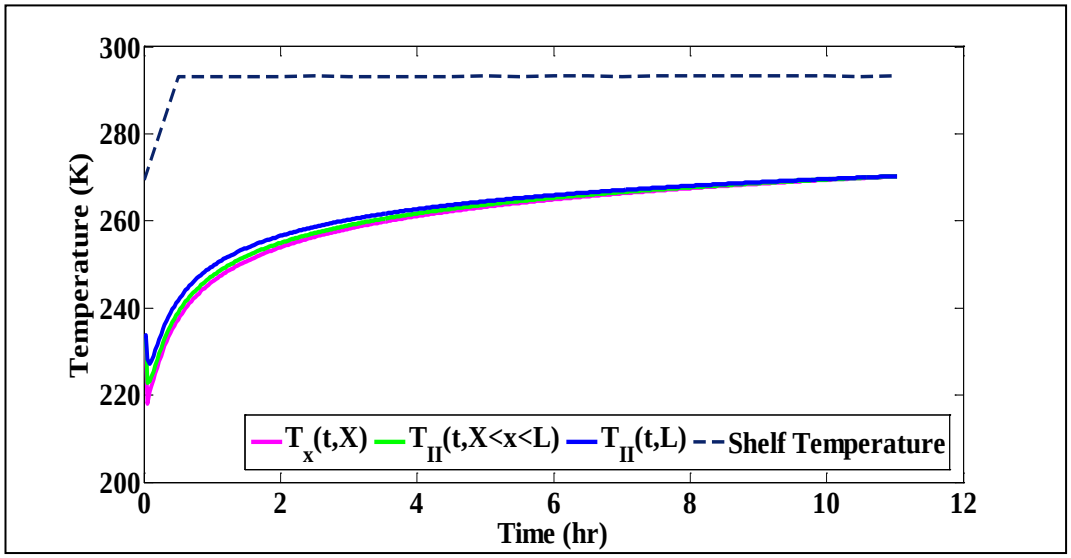

Figure 4.6: Profiles for the product temperature evaluation in time at different sample positions of frozen layer for 12.4 mm thick turkey meat slab.

In Figure 4.7, the experimental and predicted temperature profiles (also the temperature of the moving interface) for 12.4 mm thick turkey breast meat slabs during primary drying stage are presented. The experimental center point temperature $T_{exp}(t, L/2)$, data during the primary drying stage is close to the temperature of the moving interface, T_x, approximately between the hours of 4.2-6.0. It is possible to determine that experimental center point data is close to the interface temperature when the moving interface pass through the half of the thickness (Figure

4.7 and 4.9). After this time interval, the two temperature lines diverge. The center point is situated in dried region and $T_{exp}(t, L/2)$, is higher than the interface temperature (Figure 4.7). It is impractical to determine accurately the interface temperature from thermocouple sensors inserted at various spatial positions of the product being freeze-dried in trays (bulk freeze-drying) or in vials [Liapis et al., 1996]. Because the position of interface does not stay constant, it moves as drying proceeds. The best way for determining the product temperature by minimizing human intervention that is required for pharmaceutical industry is to use accurate and robust procedure such as validated mathematical models.

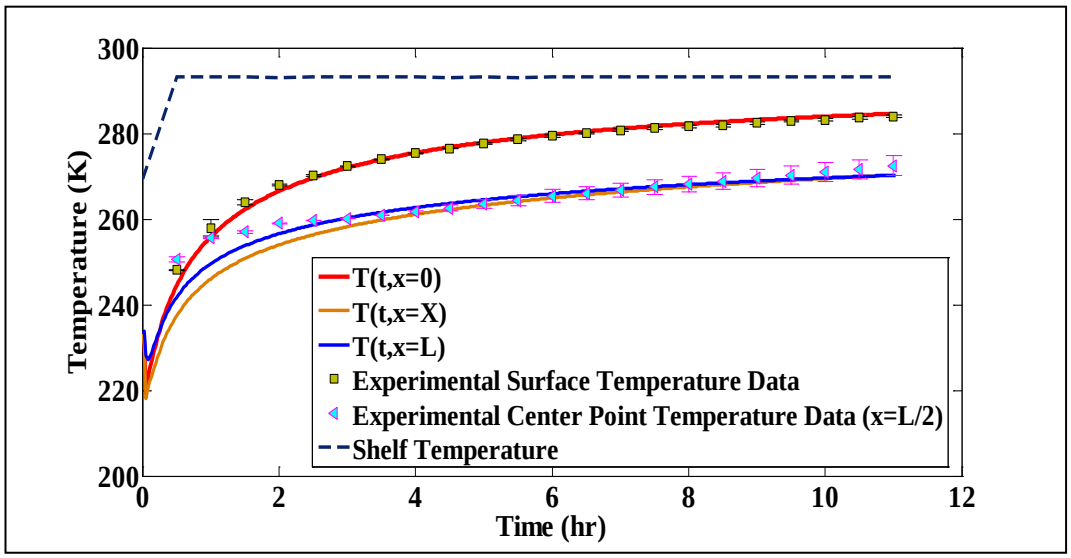

Figure 4.7: Profiles for the product temperature evaluation in time at positions x=0, x=X and x=L and comparison of experimental product surface temperature during primary drying stage for 12.4 mm thick turkey meat slab.

Figure 4.8 shows experimental and predicted temperature profiles for 12.4 mm thick turkey meat slabs during primary and secondary drying stage. The mean values of the two experimental surface and center point temperatures are plotted together with the error bars representing the maximum deviations with respect to the mean values. The mean value of the experimental surface temperature, $T_{exp}(t, 0)$, shows reasonable agreement with theoretical temperature results of turkey breast meat product during primary and secondary drying stage. The mean value of the experimental center point temperature data show a good agreement during primary drying stage.

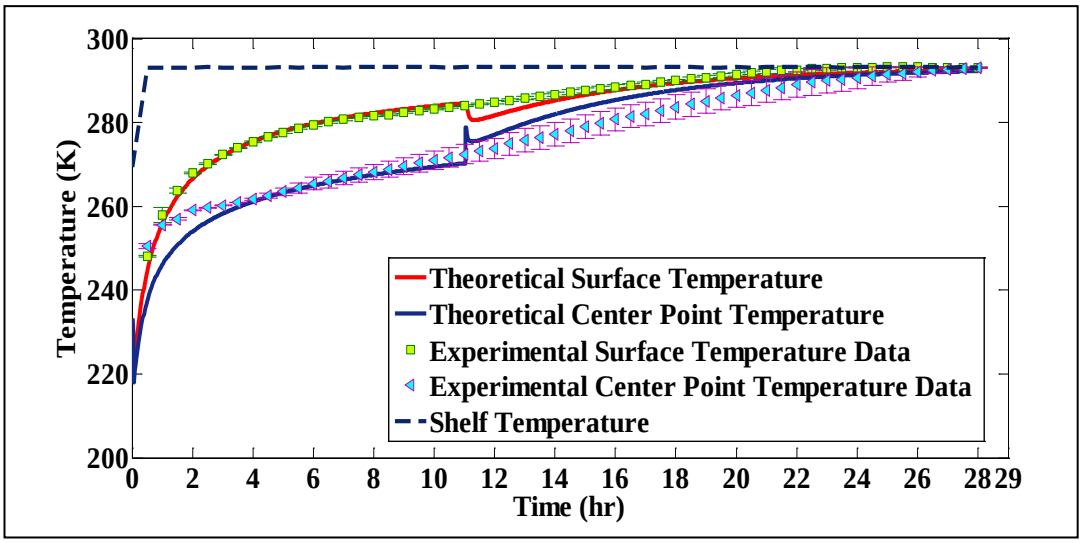

Figure 4.8: Profiles for the product temperature evaluation in time at positions x=0 and x=L/2 and comparison of experimental product surface temperature during primary and secondary drying stage for 12.4 mm thick turkey breast meat slab.

In the process of freeze-drying, as the ice is sublimating, the interface between the dried layer and the frozen layer which started at the outer surface of product, will be continuously moving backward. The position of the sublimation interface and water vapor mass flux, $(N_w(t,X))$, at different times during the primary drying stages of meat product is presented in Figure 4.9. The direction of the water vapor mass flux is in the opposite direction to that taken to represent the positive direction in the dried layer of the material being dried. At the start of the primary drying stage, the water vapor mass flux has its maximum value because resistance to mass transfer is negligible since the thickness of the dried layer has a rapid increase and provides a significant resistance to mass and heat transfer [Kochs et al., 1993], and later on the water vapor mass flux decreases smoothly until the end of the primary drying stage. The driving force of the vapor flow is the vapor pressure difference between the moving interface and the cold surface of the condenser [Hua et al., 2010].

In Figure 4.10, the experimental data and the theoretical results for water removed are presented. The theoretical results for water removed data, obtained by solution of the mathematical models with the best fit parameters, are in good agreement with the experimental water removed data. The maximum experimental uncertainty in the measurement of the meat sample weights is ±0.433 g. By considering the difficulty and complexity of the freeze-drying process during the primary drying stage, presented model correctly predicted the dynamic behavior of

the freeze-drying of turkey breast meat. The presented model involves the removal of frozen water by sublimation and the removal of unfrozen water by desorption in the dried layer during primary drying stage.

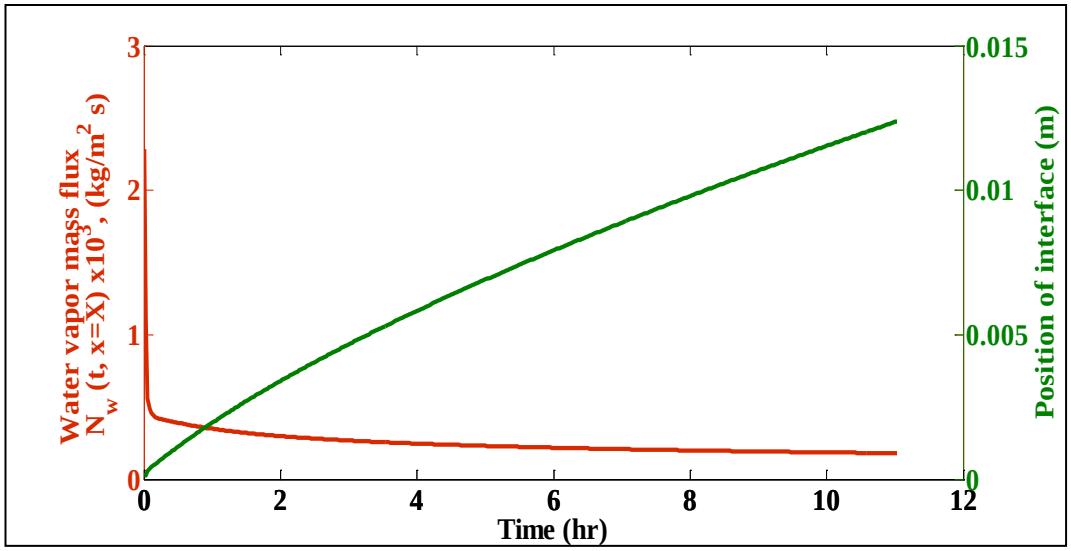

Figure 4.9: Position of the moving interface and water vapor mass flux vs. time during the primary drying stage for 12.4 mm thick turkey breast meat slab.

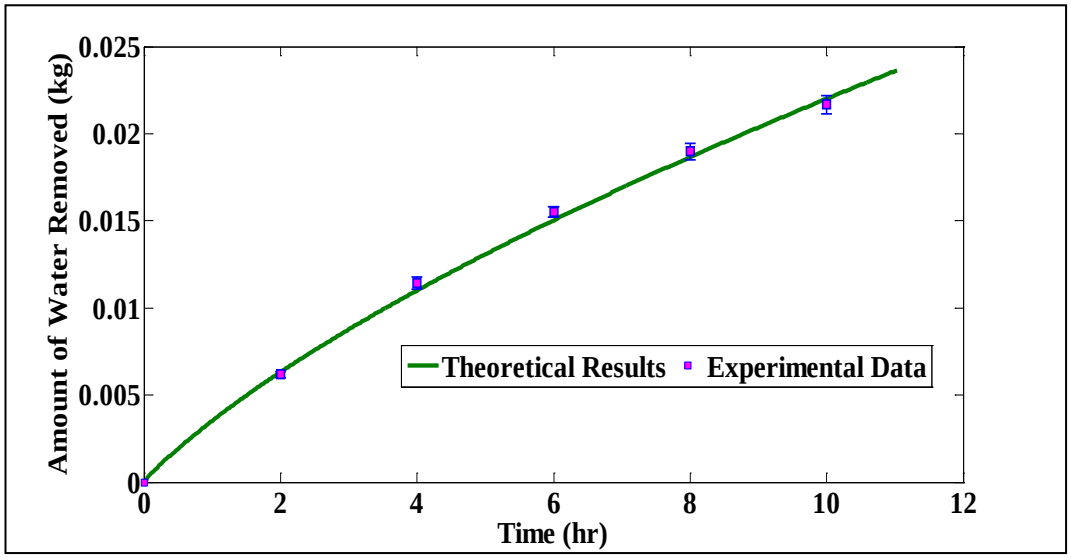

Figure 4.10: Amount of removed water vs. time during the primary drying stage of freeze-drying of turkey meat for 12.4 mm thick turkey breast meat slab.

The removal of bound water during the primary drying stage is presented in Figure 4.11. 2.53 % of the initial amount of bound water in the meat product is removed during primary drying stage. According to [Sadikoglu and Liapis, 1997] as

a result of low water vapor concentration gradient found inside the pore matrix, contribution of desorption of bound water to total mass flux of water removed during primary drying is not significant. As most of the water during primary drying stage is produced by sublimation of the frozen water, the positive relationship can be observed between interface moving rate and amount of removed water (Figure 4.9 and 4.10). Predicted by theoretical model and confirmed by the experimental data that 88.1% of the total water content of turkey breast meat was removed during the primary drying stage.

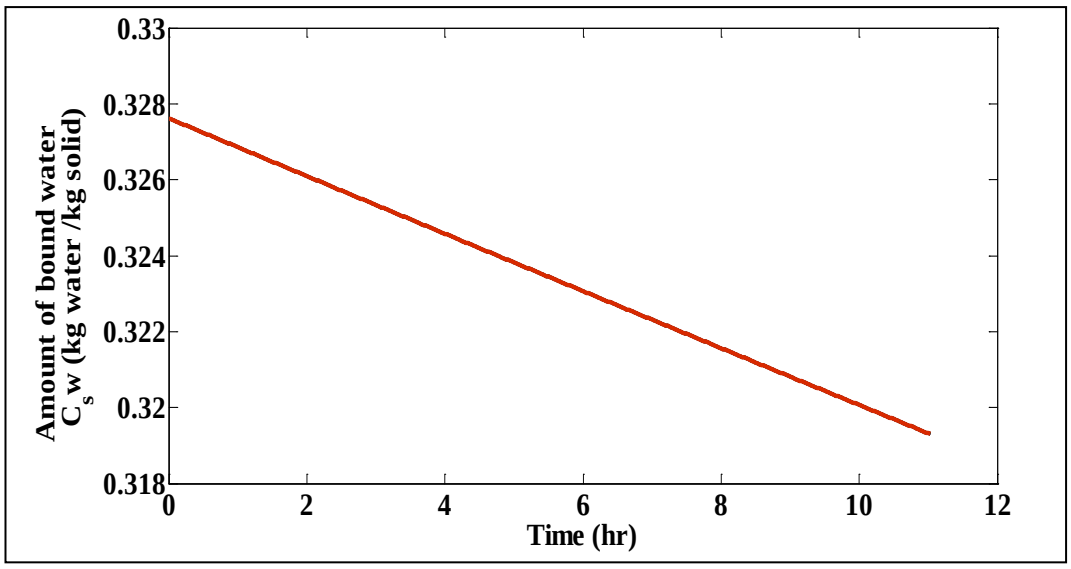

Figure 4.11: Amount of bound water vs. time during the primary drying stage of turkey meat for 12.4 mm thick turkey breast meat slab.

Figure 4.12 shows the amount of water remaining in the meat sample at various drying times during the secondary drying stage. The secondary drying stage of the turkey breast meat slab begins at about the eleven hours after start of the primary drying stage and lasts about seventeen hours. The major objective of secondary drying is to reduce the residual moisture content to an optimal level for stability which is usually between 2% to 5% for food products. The residual moisture amount in the product is coincidence with the bound water content all along the secondary drying stage, as the contribution of the removal of bound water to the total mass flux of water removed during the secondary drying stage is dominant [Sadikoglu and Liapis, 1997]. Knudsen diffusion, bulk diffusion, and convective flow are considered in the mechanisms of mass transfer of water vapor and inert gas in the pores of the dried layer during the secondary drying stage. The linear rate mechanism given in

equation (3.14) could describe satisfactorily the removal of bound water during the secondary drying stage. The best fitted parameters of desorption rate constant, k_d, Knudsen diffusivity constant for water vapor, K_w, film thermal conductivity constant, k_f, and effective thermal conductivity constant of the porous dried layer k_{Ie}, are employed in the mathematical model for the secondary drying stage to obtain the theoretical data for the residual water inside pores of the sample. Then, the theoretical results and experimental data for the amount of residual water in the sample at various drying times is compared and the agreement between the experimental and theoretical data in Figures 4.12 is, for all practical purposes, good.

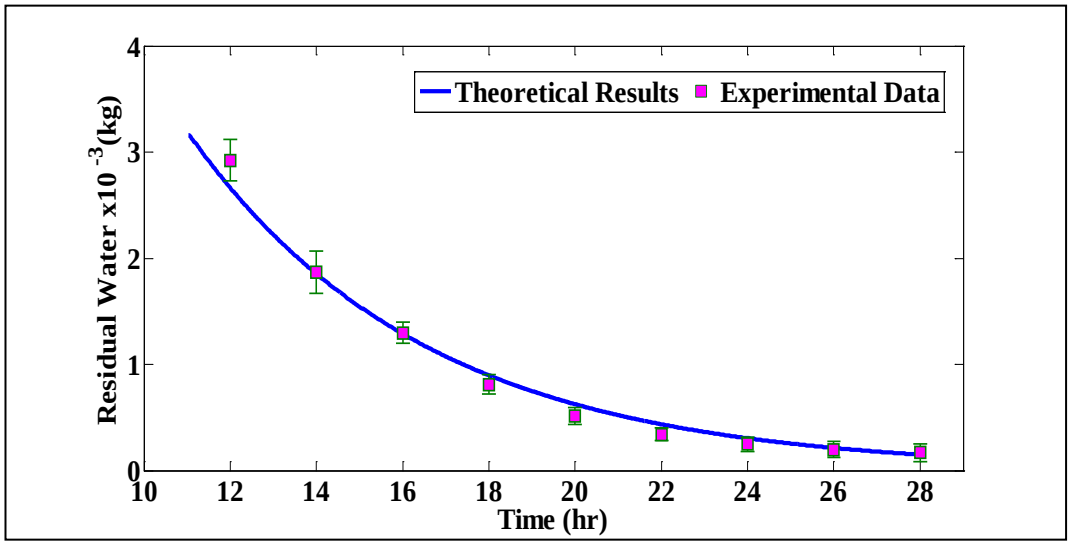

Figure 4.12: Amount of residual water vs. time during the secondary drying stage of turkey meat for 12.4 mm thick turkey breast meat slab.

In order to validate the results presented in this work, the dynamic mathematical model solved for 14.5 mm thickness of turkey breast meat slab along with the best fitted parameters of desorption rate constant, Knudsen diffusivity constant for water vapor, film thermal conductivity constant and effective thermal conductivity constant of the porous dried layer. The value of the squared 2-norm of the residual (called resnorm in Matlab) was found 2.2794×10^{-5}. In Figures 4.13, the experimental data and the theoretical results for the amount of water removed from the turkey breast meat slab with two different thicknesses of 12.4 and 14.5 mm, at various drying times, during entire duration of freeze-drying process, is shown. Figure 4.13 clearly shows that the given mathematical model can be used to predict

dynamic behavior of freezing drying of turkey breast meat slab in trays of freeze dryer.

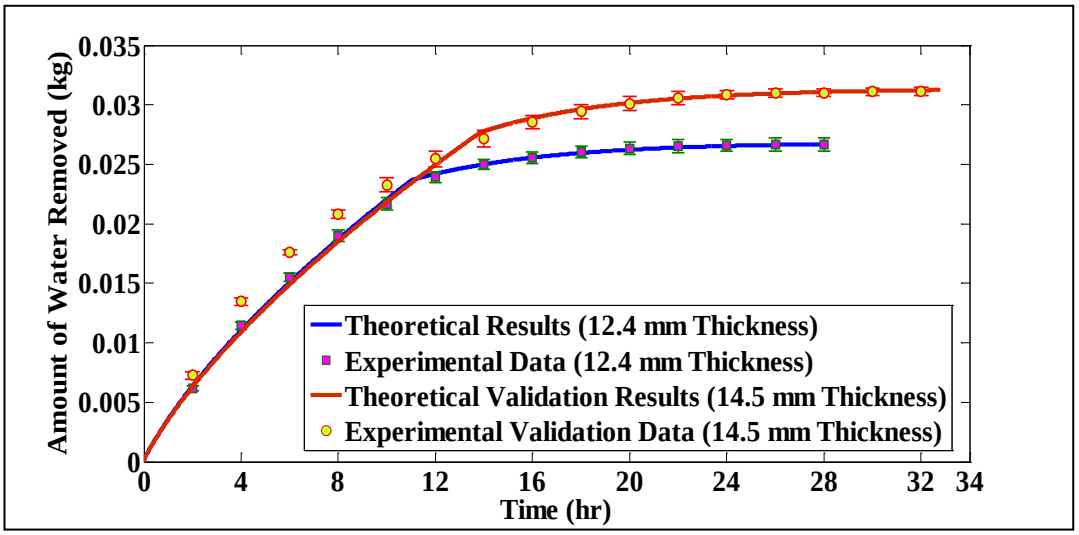

Figure 4.13: Amount of water removed versus time during the duration of the freeze-drying of turkey breast meat slab in trays for different sample thicknesses.

5. CONCLUSION

The analyses show that trends in the world on foods increasingly give importance to consumer demands for food products with minimal processing and high quality. While freeze-drying is considered to be an alternative process to preserve foods, high operating costs have limited the application of freeze-drying in the food industry. Models on freeze-drying for foodstuffs play important role to reduce processing time and energy consumption.

In order to describe quantitatively the dynamic behavior of the primary and secondary drying stages of the freeze-drying of turkey breast meat in trays, a modified mathematical model was established and solved. Some transport parameters and physical properties that characterize freeze-drying of turkey breast meat were determined by fitting experimental data with the mathematical model using non-linear least square method of Levenberg-Marquardt algorithm of MATLAB. The theoretical results that are obtained with the best fitted transport parameters were compared with the experimental data that were obtained from freeze-drying of turkey breast meat by using a pilot scale freeze-drier. It was found that the agreement between the experimental data and the results obtained from the theoretical model is, for all practical purposes, good. To verify the reliability of the resented mathematical model, the dynamic mathematical model solved for 14.5 mm thickness of turkey breast meat slab along with the best fitted parameters of desorption rate constant, Knudsen diffusivity constant for water vapor, film thermal conductivity constant and effective thermal conductivity constant of the porous dried layer. The results obtained in this study support the expectations based on the model and show that the mathematical model represents well the process. This dynamic model would be considered as a useful tool for optimization of the freeze-drying process. As there are limited number of researches in the design, optimization and control of the freeze-drying process in foodstuffs, the number of further researches is expected to increase.

6. RECOMMENDATIONS

This present study focuses mainly on the modeling and parameter estimation of the freeze-drying of turkey breast meat. The changes in quality of breast meat weren’t measured and it is possible to conduct further research in this area to understand the effect of freeze-drying process parameters on quality of turkey breast meat and validate the effectiveness of process to the product quality.

REFERENCES

Ashrae (2006), “Thermal Properties of Foods.” In: “American Society of Heating, Refrigeration and Air-Conditioning Engineers Handbook: Refrigeration”, Amer Society of Heating.

Berk Z., (2009), “Freeze-Drying (Lyophilization) and Freeze Concentration.” In: Z. Berk, Editor, “Food Process Engineering and Technology”, Academic Press.

Boss E. A., Filho R. M., de Toleda E. C. V., (2004), “Freeze drying process: real time model and optimization”, Chemical Engineering and Processing, 43, 1475-1485.

Chakraborty R., Saha A. K., Bhattacharya P., (2006), “Modeling and simulation of parametric sensitivity in primary freeze-drying of foodstuffs”, Separation and Purification Technology, 49, 258-263.

Daraoui N., Dufour P., Hammouri H., Hottot A., (2010), “Model predictive control during the primary drying stage of lyophilisation”, Control Engineering Practice, 18, 483-494.

DeMan J. M., (1999), “Principles of Food Chemistry”, 3th Edition, Aspen Publisher.

Dolan J. P., (1998), “Use of Volumetric Heating to Improve Heat Transfer During Vial Freeze-Drying”, Doctoral Thesis, Virginia Polytechnic Institute.

Fey Y. C., Boles M. A., (1988), “Analytical study of vacuum sublimation in an initially partially filled frozen porous medium with recondensation”, International Journal of Heat and Mass Transfer, 36 (7), 1727-1738.

Ghosh P., (2006). “Numerical Methods with Computer Programs in C++”, 1st Edition, Prentice-Hall of India.

Gieseler H., (2004), “Product Morphology and Drying Behavior Delineated by a New Freeze-Drying Microbalance”, Doctoral Thesis, University of Nuremberg-Erlangen.

Hua T. C., Liu B. L., Zhang, H., (2010). “Freeze-Drying of Pharmaceutical and Food Products”, 1st Edition, CRC Press.

James S. J., James C., (2002), “Meat Refrigeration”, 6th Edition, Woodhead Publishing.

Jennings T. A., 2008, “Lyophilization: Introduction and Basic Principles”, 1st Edition, Informa Healthcare.

Kasper J. C., Friess W., (2011), “The freezing step in lyophilization: physico-chemical fundamentals, freezing methods and consequences on process performance

and quality attributes of biopharmaceuticals", European Journal of Pharmaceutics and Biopharmaceutics, 78, 248-263.

Khalloufi S., Robert J. L., Ratti C., (2005), "Solid foods freeze-drying simulation and experimental data", Journal of Food Process Engineering, 28, 107-132.

King C. J., (1970), "Freeze drying of foodstuff", Critical Reviews in Food Science and Technology", 1 (3), 379-451.

Kochs M., Körber C. H., Heschel I., Nunner B., (1993), "The influence of the freezing process on vapour transport during sublimation in vacuum-freeze-drying of macroscopic samples", International Journal of Heat and Mass Transfer, 36 (7), 1727-1738.

Kuu W. Y., McShame J., Whong J., (1995), "Determination of mass transfer coefficients during freeze drying using modeling and parameter estimation techniques", International Journal of Pharmaceutics, 124 (2), 241-252.

Liapis A. I., Bruttini R., (2006), "Freeze-Drying". In: A. S. Mujumdar, Editor, "Handbook of Industrial Drying", CRC Press.

Liapis A. I., Bruttini R., (2009), "A mathematical model for the spray freeze drying process: the drying of frozen particles in trays and in vials on trays", International Journal of Heat and Mass Transfer, 52, 100-111.

Liapis A. I., Litchfield R. J., (1979), "Numerical solution of moving boundary transport problems in finite media by orthogonal collocation", Computers & Chemical Engineering, 3, 615-621.

Liapis A. I., Pikal M. J., Bruttini R., (1996), "Research and development needs and opportunities in freeze-drying", Drying Technology, 14 (6), 1265-1300.

Litchfield R. J., Farhadpour F. A., Liapis A. I., (1981), "Cyclical pressure freeze drying", Chemical Engineering Science, 36, 1233-1238.

Litchfield R. J., Liapis A. I., (1979), "An adsorption-sublimation model for a freeze dryer", Chemical Engineering Science, 34, 1085-1090.

Litcfield R. J., Liapis A. I., (1982), "Optimal control of a freeze dryer-II: dynamic analysis", Chemical Engineering Science, 37, 45-55.

Lombrana J. I., (2008), "Fundamentals and Tendencies in Freeze-Drying of Foods". In: C. Ratti, Editor, "Advances in Food Dehydration", CRC Press.

Lopez-Quiroga E., Antelo L. T., Alonso A. A., (2012), "Time-scale modeling and optimal control of freeze-drying", Journal of Food Engineering, 111, 655-666.

Mason E. A. and Malinauskas, A. P., (1983), "Gas Transport in Porous Media –The Dusty Gas Model", 1st Edition, Elsevier.

Mellor J. D., (1978), “Fundamentals of Freeze-Drying”, 1st Edition, Academic Press.

Millman M. J., Liapis A. I., Marchello J. M., (1985), “An Analysis of The Lyophilization Process Using a Sorption-Sublimation Model and Various Operational Policies”, AIChe, 31 (10), 1594-1604.

Nesvadba P., (2008). “Thermal Properties and Ice Crystal Development in Frozen Foods”. In: J.A. Evans, Editor: “Frozen Food Science and Technology”, Wiley Blackwell.

Oetjen G., Haseley P., (2004), “Freeze-Drying”, 2nd Edition, Wiley-Vch.

Pikal M. J., Shah S., (1990), “The collapse temperature in freeze-drying: dependence on measurement methodology and rate of water removal from the glass phase”, International Journal of Pharmaceutics, 62, 165-186.

Pikal M. J., Shah S., Roy M. L., Putman R., (1990), “The secondary drying stage of freeze-drying: drying kinetics as a function of temperature and chamber pressure”, International Journal of Pharmaceutics, 60, 203-217.

Rahman M. S., (2006), “State diagram of foods: Its potential use in food processing and product stability”, Trends in Food Science & Technology, 17, 129-141.

Ramirez W. F., (1997), “Computational Methods for Process Simulation”, 2nd Edition, Butterworth-Heinemann.

Ratti C., (2001), “Hot air and freeze-drying of high-value foods: A review”, Journal of Food Engineering, 49, 311-319.

Ratti C., (2012), “Freeze-Drying Process Design”. In: J. Ahmed, M. S. Rahman, Editors, “Handbook of Process Design”, Blackwell Publishing.

Sadikoglu H., (1998), “Dynamic Modeling and Optimal Control of the Primary and Secondary Drying Stages of Freeze Drying of Solutions in Trays and Vials” Doctoral Thesis, University of Missouri-Rolla.

Sadikoglu H., Liapis A. I., (1997), “Mathematical modeling of the primary and secondary drying stages of bulk solution freeze-drying in trays: parameter estimation and model discrimination by comparison of theoretical results with experimental data”, Drying Technology, 15, 791-810.

Sadikoglu H., Liapis A. I., Crosser O. K., Bruttini R., (1999), “Estimation of the effect of product shrinkage on the drying times, heat input and condenser load of the primary and secondary drying stages of the lyophilization process in vials”, Drying Technology, 17 (10), 2013-2035.

Sadikoglu H., Ozdemir M., Seker M., (2006), “Freeze-drying of pharmaceutical products: research and development needs”, Drying Technology, 24 (7), 849-861.

Sandall O. C., King J., Wilke C. R., (1967), “The relationship between transport properties and rates of freeze-drying of poultry meat”, AIChE Journal 13 (3), 428-438.

Searles J. A., (2010), “Freezing and Annealing Phenomena in Lyophilization”. In: L. Rey, J. C. May, Editors, “Freeze-drying/Lyophilization of Pharmaceutical and Biological Products”, Informa Healthcare.

Singh R. P., Sarkar A., (2005), “Thermal Properties of Frozen Foods”. In: M. A. Rao, A. K. Datta, S. H. Rizvi, Editors, “Engineering Properties of Foods”, CRC Press.

Stapley A..(2008), “Freeze Drying”. In: J.A. Evans, Editor: “Frozen Food Science and Technology”, Wiley Blackwell.

Valdes-Fragaso A., Arguilles-Pina L. D., Martinez Garcia, O., Mujica-Paz, H., (2008), “Freeze Drying of Meats and Seafood.” In: Y. H. Hui, Editor: “Food Drying Science and Technology: Microbiology, Chemistry, Applications”, Destech Publications.

Velardi S. A., Barresi A. A., (2008), “Development of simplified models for the freeze-drying process and investigation of the optimal operating conditions”, Chemical Engineering Research and Design, 86, 9-22.

Villadsen J., Michelsen M. L., (1978), “Solution of Differential Equation Models by Polynomial Approximation”, 1st Edition, Prentice Hall.

Welti-Chanes J., Vergara-Balderas F., Perez-Perez E., Reyes-Herrera A., (2005), “Fundamentals and new tendencies of freeze-drying foods”, Segundo Simposio International de Innovacion Desarrollo de Alimentos, 31-47, Montevideo, Uruguay, 28-30 Septiembre.

Wiklund E., Kemp R. M., Leroux G. J., Li Y., Wu G., (2010), “Spray chilling of deer carcasses-effects on carcass weight, meat moisture content, purge, and microbiological quality”, Meat Science, 86, 926-930.

Yalçın Y. M., (2014), “Dondurarak Kurutucu Kullanılarak Üretilen Tuzlanmış ve Baskılanmış Hindi Etinin Bazı Fiziksel Özelliklerinin İncelenmesi”, Yüksek Lisans Tezi, Gebze Yüksek Teknoloji Enstitüsü.

BIOGRAPHY

Öznur Cumhur, was born in 1983 in Sakarya. She graduated from Sakarya Anatolian High School in 2001 and from the Faculty of Food Engineering of Hacettepe University in 2006. She gained postgraduate scholarship from The Scientific and Technological Research Council of Turkey (TUBİTAK), the program 2228. She got her master degree in Food Engineering from İstanbul Technical University, 2008. She worked as a project assistant in a TUBİTAK project during post graduate education. She has been a doctoral student in the Department of Chemical Engineering at Gebze Technical University. She has been working as a specialist at Bilecik Şeyh Edebali University.

APPENDICES

Appendix A: Article within the Scope of Thesis

Cumhur Ö., Şeker M., Sadıkoğlu H., "Freeze-Drying of Turkey Breast Meat: Mathematical Modeling and Estimation of Transport Parameters", Drying Technology (DOI: 10.1080/07373937.2015.1064945).

Appendix B: Matlab Code for Mathematical Modeling of Turkey Meat

Table B1.1: Matlab Main Function File for Primary and Secondary Drying Stage.

```
%%%%%%%%%%%%%%%%%%%%%%%%%%%%%%%%%%%%%%%%%%%%%%%%%%
%%%%%%%%%%%%%%%%%%%%%%%%%%%%%%%%%%%%%%%%%%%%%%%%%%
% GEBZE TECHNICAL UNIVERSITY
% DEPARTMENT OF CHEMICAL ENGINEERING
%  PROGRAM TO SOLVE THE MATHEMATICAL MODEL OF MEAT
FREEZE-DRYING IN TRAYS

WRITTEN BY:
OZNUR CUMHUR

ADVISORS:
PROF. DR. HASAN SADIKOĞLU
ASSOC. PROF. DR. MAHMUT SEKER
%%%%%%%%%%%%%%%%%%%%%%%%%%%%%%%%%%%%%%%%%%%%%%%%
% Matlab main.m File for Primary and Secondary Drying Stage
clc
clear
global X X1 X2 A B A1 A2 B1 B2 n q LEN KSI
global RHO1 RHO1E RHO2 WMWT AMWT PIN PWO PC   PTT VIS KW KI
KMX CO1 C2 CO CSWE DOWIN KBULKW KSELF KBULKI SIG KD KS R
EF K2 KF K1E TAP TUP FAK CPG CP1 CP2 DHS DHV TMELT TSCOR
TBAS TYUZ TARA TALT TORT TORT2 NW
```

Table B1.1: Continued.

```
n=10; % "Collocation Points (including boundary points)"
TBAS=233.15; % "Freezing Temperature (K)"
PWO=1.07; % "Initial Water Vapor Pressure at the Surface (N/m^2)"
%"After parameter estimation constant values used. "
constant1=1.04;
CO=0.315*constant1;%"Weight Fraction of Bound Water in Dried Layer (kg water / kg solid)"
[X, A, B, q] = colloc (n-2, -0.5, 'left', 'right');
LEN=0.0124;       %" Sample Thickness (m)"
ALANY=0.0730*0.0330;   % "Area of the Sample"
iwa=(26.8485/1000); %" Amount of Initial Water"
KSI=0.01*LEN;  %" Initial Interface Position"
% Scaling, (1-Dried Layer ) (2- Frozen Layer)
X1=X*KSI; % "Dried Layer Collocation Points"
X2=(LEN-KSI)*X+KSI; % "Frozen Layer Collocation Points"
A1=A/KSI; %" Matrice of A for Dried Layer "
A2=A/(LEN-KSI); % "Matrice of A for Frozen Layer "
B1=B/(KSI*KSI); % "Matrice of B for Dried Layer "
B2=B/((LEN-KSI)*(LEN-KSI)); % "Matrice of B for Frozen Layer"
% "Initial Boundary Conditions "
T0=zeros(2*n,1)+TBAS;
T0(2*n+1:3*n)=PWO;
T0(3*n+1:4*n)=CO;
T0(4*n+1)=KSI;
T0dot=zeros(4*n+1,1);
NW1=[ ];
NW2=[ ];
T1=T0'; %"To create Index"
timet=0;
timet2=0;
j=0;
REMW(j+1)=0;
```

Table B1.1: Continued.

```
NWN(j+1)=0;
OF2=0.0;
io=0.0;
for i=1:100:90001 % "Time Cycle for Primary Drying Stage"
   tstop=i;
   nts=3; % "Step in the time range "
   tsteps=linspace(io, tstop, nts)'; % "Time range"
   j=j+1;
   opts = odeset ('AbsTol',1,'RelTol',1);
[tout, T] = ode15i (@heateq, tsteps, T0, T0dot, opts); %"Calling heateq file for
Primary Drying Stage"
NW1=[NW1;NW']; % "Total Mass Flux "
times=i;
timet=[timet, times'];
REMW(j+1)=-NW(n)*ALANY*(i-io)+REMW(j); %" Amount of Removed
Water for Primary Drying Stage "
OF2=NW(n);
KSI=T(3,4*n+1);
X1=X*KSI;
X2=(LEN-KSI)*X+KSI;
A1=A/KSI;
A2=A/(LEN-KSI);
B1=B/(KSI*KSI);
B2=B/((LEN-KSI)*(LEN-KSI));
if KSI>(0.999*LEN), break, end %" End of the Primary Drying Stage "
T0=T(3,:)';
T1=[T1; T(3,:)];
io=i;
end
pdt=tstop/3600     %"Primary Drying Stage Time"
% "Secondary Drying Stage"
T00(1:n)=T1(end,1:n)';
```

Table B1.1: Continued.

```
T00(n+1:2*n)=T1(end,2*n+1:3*n)';
T00(2*n+1:3*n)=T1(end,3*n+1:4*n)';
T0dot=zeros(3*n,1);
T2=T00;
j2=0;
REMWS(j2+1)=0;
io2=0;
for i2=1:100:100001 %"Time Cycle for Secondary Drying Stage"
    tstop=i2;
    tsteps=linspace(io2, tstop, 3)';
     j2=j2+1;
opts = odeset ('AbsTol',1,'RelTol',1D-1);
[tout, T] = ode15i (@heateq2, tsteps, T00, T0dot, opts); %"Calling heateq2.file
for Secondary Drying Stage"
NW2=[NW2;NW'];
times2=i2;
timet2=[timet2; times2'];
REMWS(j2+1)=REMWS(j2)-NW(1)*ALANY*(i2-io2);  % "Amount of
Removed Water"
REMWB2(j2)=(iwa-REMW(end))-REMWS(j2);   % "Amount of  Residual
Water"
if REMWB2(j2)<=1.5e-4 break, end % "End of the Secondary Drying Stage"
T00=T(3,:)';
T2=[T2; T(3,:)];
io2=i2;
if T2(end,3*n)<=0.01  break, end
end
sdt=tstop/3600   %"Secondary Drying Stage Time"
```

Table B1.2: Matlab "heateq.m" File for Primary Drying Stage.

```
%Primary Drying Stage Matlab heateq.m File
function resid = heateq(t, T, Tdot)
global X X1 X2 A B A1 A2 B1 B2 n LEN KSI
global RHO1 RHO1E RHO2 WMWT AMWT PIN PWO PC PWX PWW PTT
VIS KW KI KMX CO1 C2 CO CSWE DOWIN KBULKW KSELF KBULKI
SIG KD KS R EF OM K2 KF K1E TAP TUP FAK CPG CP1 CP2 DHS DHV
TMELT TSCOR TBAS TYUZ TARA TALT TORT TORT2 NW
resid=zeros(4*n+1,1);
% "Expressions and Values of the Physical and Transport Properties"
TMELT=263.84;  %" Melting Temperature (K)"
TSCOR=333.15;  % "Scorch Temperature (K)"
TBAS=233.15; % "Freezing Temperature (K)"
TYUZ=T(1,1); % "Upper Dried Surface Temperature (K)"
TARA=T(n,1); % "Moving Interface Temperature (K)"
TALT=TBAS; % "Bottom Surface of Product Temperature (K)"
TORT=(TARA+TYUZ)/2; % "Average Temperature in the Dried Layer (K)"
TORT2=(TARA+TALT)/2; % "Average Temperature of Frozen Layer (K)"
TAP=293.15; % "Lower Plate Temperature (K)"
TUP=293.15; %" Upper Plate Temperature (K)"
PIN=PC-PWO; % "Initial Inert Gas Pressure (N/m^2)"
PWO=1.07; % "Initial Water Vapor Pressure at the Surface (N/m^2)"
PC=10; % "Chamber Pressure (N/m^2)"
R=8314; % "İdeal Gas Constant (J/kg mol*K)"
WMWT=18; % "Molecular Weight of Water (kg/kg mol)"
AMWT=28.82; % "Molecular Weight of Air (kg/kg mol)"
RHO1=333;  %" Density of Dried Layer (kg/m^3) "
RHO2=1133;  % "Density of Frozen Layer (kg/m^3) "
RHO1E=RHO1; %" Effective  Density of Dried Layer (kg/m^3)"
EF=0.74; % "Voidage Fraction "
DHS=2840; % "Enthalpy of Sublimation of Frozen Water (kJ/kg)"
DHV=2687.4; % "Enthalpy of Vaporization of Bound Water (kJ/kg)"
CPG=1.6166; %" Heat Capacity of Gas (kJ/kg K)"
```

Table B1.2: Continued.

```
CP1=((23.948*(4.1762-(0.000090864*(TORT-273.15))+(0.0000054791*(TORT-273.15)*(TORT-273.15))))+(59.870*(2.0082+(0.0012089*(TORT-273.15))-(0.0000013129*(TORT-273.15)*(TORT-273.15))))+
(13.523*(1.9842+(0.0014733*(TORT-273.15))- (0.0000048008*(TORT-273.15)*(TORT-273.15))))+ (2.660*(1.0926+(0.0018896*(TORT-273.15))-(0.0000036817*(TORT-273.15)*(TORT-273.15)))))/100; % "Effective Heat Capacity of Dried Layer (kJ/kg K)"
CP2=((74.838*(2.0623+(0.0060769*(TORT2-273.15))))
+(19.808*(2.0082+(0.0012089*(TORT2-273.15))-(0.0000013129*(TORT2-273.15)*(TORT2-273.15))))+(4.474*(1.9842+(0.0014733*(TORT2-273.15))-(0.0000048008*(TORT2-273.15)*(TORT2-273.15))))+
(0.88*(1.0926+(0.0018896*(TORT2-273.15))-(0.0000036817*(TORT2-273.15)*(TORT2-273.15)))))/100; % "Heat Capacity of Frozen Layer (kJ/kg K)"
PWX=133.3224*exp(-2445.5646./T(n,1)+8.2312*log10(T(n,1))-0.01677006*T(n,1)+1.20514e-5.*T(n,1)*T(n,1)-6.757169); %" PWX=F(Tx) Water Vapor Pressure-Temperature Functional Form Presented (N/m^2)"
PWW=(PWX+PWO)./2; % "Average Water Vapor Pressure in the Dried Layer (N/m^2)"
PTT=PIN+PWW; %" Average Pressure in the Dried Layer (N/m^2)"
VIS=18.4858E-7*((TORT^1.5)/(TORT+650)); %" Viscosity (kg/m s)"
CO1=7.219e-15;  % "Constant Dependent Only upon structure of Porous Medium and Giving Relative Darcy Flow Permeability (m^2)"
C2=0.19; % "Constant Dependent Only Upon Structure of Porous Medium and Giving the Ratio of Bulk Diffusivity within the Porous Medium to the Free Gas Bulk Diffusivity "
%"Knudsen Diffusivity for Water Vapor, (m^2/s)"
constant2=0.19;
KW=(1.6395e-4*(TYUZ+TARA)^0.5)*constant2;
KI=1.126D-4*(TYUZ+TARA)^0.5; % "Knudsen Diffusivity(Inert Gas), (m^2/s)"
"KMX=(PWW./PTT).*KI+(PIN./PTT).*KW; % "Weighted Average Knudsen Diffusivity for Binary Gas Mixture, (m^2/s)"
```

Table B1.2: Continued.

```
K2=0.48819/TALT+(0.4685e-3);  % "Thermal Conductivity of Frozen Layer (kW / K m)"
% "Film Thermal Conductivity (kW/m^2 K)"
constant3=1.34;
KF=(1.5358e-3*PC)*constant3;
% "Effective Thermal Conductivity of Dried Layer (kW/K m)"
constant4=0.52;
K1E(1:n,1)=constant4*85e-6*(1-(0.325*exp(-5e-3*PTT)));
DOWIN=8.729e-7*((TYUZ+TARA)^2.334);  % "Free Gas Mutual  Diffusivity in a Binary Mixture Of Water Vapor and Inert Gas (kg m/s^3)"
KBULKW=C2*DOWIN*KW/(C2*DOWIN+KMX*(PIN+PWO)); % "K1= Bulk Diffusivity Constant (m^2/s)"
KSELF=KW*KI/(C2*DOWIN+KMX*(PIN+PWO))+(CO1/VIS); %"K2=K4= Self Diffusivity Constant (m^2/s)"
KBULKI=C2*DOWIN*KI/(C2*DOWIN+KMX*(PIN+PWO)); % "K3= Bulk Diffusivity Constant (m^2/s)"
KD=6.48e-7; % "Desorption Rate Constant of Bound Water for Primary Drying Stage (1/s)"
SIG=5.676e-11; %"Stefan Boltzmann Constant
FAK=1; % "View Factor of the Platen with the Sample"
% "T matrix for Primary Drying Stage
%        1-n : Dried Region Temperature at Internal Collocation Point (TI)
%   n+1-2n : Frozen Region Temperature at Internal Collocation Point (TII)
% 2n+1-3n : Water Vapor Pressure at Internal Collocation Point (Pw)
% 3n+1-4n : Sorbed Water Values at Internal Collocation Point (Csw)
%  4n+1 : Moving Interface Position (X(t)) "
%"Mass Flux of Water Vapor Equation based on Dusty Gas Model (Equation 3.61)"
NW=zeros(n,1);
NW(1:n,1)=-WMWT./(R.*T(1:n,1)).*
(KBULKW+KSELF.*T(2*n+1:3*n,1)).*(A1(1:n,:)*T(2*n+1:3*n,1));
```

Table B1.2: Continued.

```
% "Heat Transfer Equation in Dried Layer (Equation 3.59)"
resid(1:n,1)=Tdot(1:n,1)-(K1E./(RHO1E.*CP1)).*(B1*T(1:n,1))
+(CPG./(RHO1E.*CP1)).*(NW(1:n,1).*(A1*T(1:n,1)))-
((DHV.*RHO1)./(RHO1E.*CP1)).*(-KD.*T(3*n+1:4*n,1))-X1.*(-
NW(n,1)/(RHO2-RHO1)).*(A1*T(1:n,1));
% "Heat Transfer in Frozen Layer (Equation 3.60)"
resid(n+1:2*n,1)=Tdot(n+1:2*n,1)-(K2./(RHO2.*CP2)).*B2*T(n+1:2*n,1)-(X2-
1).*(-NW(n,1)/(RHO2-RHO1)).*(A2*T(n+1:2*n,1));
%" Material Balance Equation for Water Vapor  (Equation 3.67)"
resid(2*n+1:3*n,1)=Tdot(2*n+1:3*n,1)-
((KBULKW+KSELF.*T(2*n+1:3*n,1)).*(B1*T(2*n+1:3*n,1))
+KSELF.*(A1*T(2*n+1:3*n,1)).*(A1*T(2*n+1:3*n,1)))/EF
+(((RHO1.*T(1:n,1).*R)./(EF.*WMWT)).*((-KD.*T(3*n+1:4*n,1)))) -X1.*(-
NW(n,1)/(RHO2-RHO1)).*(A1*T(2*n+1:3*n,1));
% "The Desorption Rate of Bound Water in the Dried Layer (Equation 3.69)"
resid(3*n+1:4*n,1)=Tdot(3*n+1:4*n,1)+(KD.*T(3*n+1:4*n,1))-X1.*(-
NW(n,1)/(RHO2-RHO1)).*(A1*T(3*n+1:4*n,1));
% "The Velocity of the Moving Interface (Equation 3.70)"
resid(4*n+1,1)=Tdot(4*n+1,1)+ NW(n,1)/(RHO2-RHO1);
% "Boundary Conditions"
resid(1)=-K1E(1)*A1(1,:)*T(1:n,1)-(SIG*FAK*(TUP.^4-TYUZ.^4)); %
(Equations 3.72 and 3.73)
resid(n)=-K2*A2(1,:)*T(n+1:2*n,1)+K1E(n)*A1(n,:)*T(1:n,1)-((-
NW(n,1)./(RHO2-RHO1))*(RHO2*CP2-RHO1*CP1)
+CPG.*NW(n))*T(n+1,1)-DHS.*NW(n);  % (Equation 3.74)
resid(n+1)=-T(n,1)+T(n+1,1);  % (Equation 3.75)
resid(2*n)=K2.*A2(n,:)*T(n+1:2*n,1)-KF*(TAP-T(2*n,1));   % (Equations 3.76
and 3.77)
resid(2*n+1)=PWO-T(2*n+1,1);    % (Equation 3.78)
resid(3*n)=PWX-T(3*n,1);        % (Equation 3.79)
```

Table B1.3: Matlab "heateq2.m" File for Secondary Drying Stage.

```
% "Secondary Drying Stage Matlab heateq2.m File"
function resid = heateq2(t, T, Tdot)
global X A B n LEN
global RHO1 RHO1E RHO2 WMWT AMWT PIN PWO PC PWX PWW PTT
VIS KW KI KMX CO1 C2 CO CSWE DOWIN KBULKW KSELF KBULKI
SIG KD KS R EF OM NW K2 KF K1E TAP TUP FAK CPG CP1 CP2 DHS
DHV TMELT TSCOR TBAS TYUZ TARA TALT TORT
resid=zeros(3*n,1);
% "Expressions and Values of the Physical and Transport Properties"
TMELT=263.15; % "Melting Temperature (K)"
TSCOR=333.15;  % "Scorch Temperature (K)"
TBAS=233.15; % "Freezing Temperature (K)"
TYUZ=T(1,1); % "Upper Dried Surface Temperature (K)"
TARA=T(n,1); %" Moving Interface Temperature (K)"
TALT=TARA; %"Bottom Surface of Product Temperature (K)"
TORT=(TARA+TYUZ)/2; % "Average Temperature in the Dried Layer (K)"
TAP=293.15; % "Lower Plate Temperature (K)"
TUP=293.15; % "Upper Plate Temperature (K)"
PWO=1.07; % "Initial Water Vapor Pressure at the Surface (N/m^2)"
PC=10; % "Chamber Pressure (N/m^2)"
PIN=PC-PWO; % "Initial Inert Gas Pressure (N/m^2)"
PWX=T(2*n,1); % "Pressure at the Bottom Surface of the Product (N/m^2)"
PWW=(PWX+PWO)/2; %"Average Water Vapor Pressure in the Dried Layer
(N/m^2)"
PTT=PIN+PWW; % "Average Pressure in the Dried Layer (N/m^2)"
EF=0.74;  % "Voidage Fraction "
R=8314; %"İdeal Gas Constant (J/kg mol*K)"
WMWT=18; %"Molecular Weight of Water (kg/kg mol)"
AMWT=28.82; %" Molecular Weight of Air (kg/kg mol)"
RHO1=333;  % "Density of Dried Layer (kg/m^3) "
RHO2=1133;  % "Density of Frozen Layer (kg/m^3) "
RHO1E=RHO1; % "Effective  Density of Dried Layer (kg/m^3)"
```

Table B1.3: Continued.

```
CPG=1.6166; % "Heat Capacity of Gas (kJ/kg K)"
% "Effective Heat Capacity of Dried Layer (kJ/kg K) "
CP1=((23.948*(4.1762-(0.000090864*(TORT-273.15))+(0.0000054791*(TORT-
273.15)*(TORT-273.15))))+(59.870*(2.0082+(0.0012089*(TORT-273.15))-
(0.0000013129*(TORT-273.15)*(TORT-
273.15))))+(13.523*(1.9842+(0.0014733*(TORT-273.15))-
(0.0000048008*(TORT-273.15)*(TORT-
273.15))))+(2.660*(1.0926+(0.0018896*(TORT-273.15))-
(0.0000036817*(TORT-273.15)*(TORT-273.15)))))/100;
DHS=2840; % "Enthalpy of Sublimation of Frozen Water (kJ/kg)"
DHV=2687.4; %" Enthalpy of Vaporization of Bound Water (kJ/kg)"
VIS=18.4858E-7*((TORT^1.5)/(TORT+650)); % "Viscosity (kg/m s)"
SIG=5.67e-11;  % "Stefan Boltzmann Constant"
CO1=7.219e-15;   % "Constant Dependent Only upon structure of Porous
Medium and Giving Relative Darcy Flow Permeability (m^2)"
C2=0.19;  % "Constant Dependent Only Upon Structure of Porous Medium and
Giving The Ratio Of Bulk Diffusivity Within The Porous Medium To The Free
Gas Bulk Diffusivity"
% "Knudsen Diffusivity for Water Vapor, (m^2/s)"
constant2=0.19;
KW=(1.6395e-4*(TYUZ+TARA)^0.5)*constant2;
KI=1.126D-4*(TYUZ+TARA)^0.5;  %" Knudsen Diffusivity (Inert Gas)
(m^2/s)"
KMX=(PWW/PTT)*KI+(PIN/PTT)*KW; % Weighted Average Knudsen
Diffusivity for Binary Gas Mixture, (m^2/s)
K2=0.48819/TALT+(0.4685e-3); %  "Thermal Conductivity of Frozen Layer
(kW / K m)"
 %" Film Thermal Conductivity (kW/m^2 K)"
constant3=1.34;
KF=(1.5358e-3*PC)*constant3;
FAK=1; % "View Factor of the Platen with the Sample"
```

Table B1.3: Continued.

```
% "Effective Thermal Conductivity of Dried Layer (kW/K m)"
constant4=0.52;
K1E(1:n,1)=constant4*85e-6*(1-(0.325*exp(-5e-3*PTT)));
DOWIN=8.729e-7*((TYUZ+TARA)^2.334);   % "Free Gas Mutual  Diffusivity
In A Binary Mixture Of Water Vapor And Inert Gas (kg m/s^3)"
KBULKW=C2*DOWIN*KW/(C2*DOWIN+KMX*(PIN+PWO)); % "K1= Bulk
Diffusivity Constant (m^2/s)"
KSELF=KW*KI/(C2*DOWIN+KMX*(PIN+PWO))+(CO1/VIS); % "K2=K4=
Self Diffusivity Constant (m^2/s)"
KBULKI=C2*DOWIN*KI/(C2*DOWIN+KMX*(PIN+PWO));   % "K3= Bulk
Diffusivity Constant (m^2/s)"
% "Desorption Rate Constant of Bound Water for Secondary Drying Stage (1/s)"
constant5=0.65;
KD=7.8e-5*constant5;
% T matrix for SECONDARY DRYING STAGE
% 1-n : Dried Region Temperature at Internal Collocation Point (TI)
% n+1-2n : Water Vapor Pressure at Internal Collocation Point (Pw)
% 2n+1-3n : Sorbed Water Values at Internal Collocation Point (Csw)
% "Mass Flux of Water Vapor Equation based on Dusty-Gas Model (Equation
3.92)"
NW(1:n,1)=-WMWT./(R.*LEN.*T(1:n,1))
.*(KBULKW+KSELF.*T(n+1:2*n,1)).*(A*T(n+1:2*n,1));
% "Heat Transfer Equation in Dried Layer (Equation 3.85)"
resid(1:n,1)=Tdot(1:n,1)-(K1E./(RHO1E.*LEN.*LEN.*CP1)).*(B*T(1:n,1))
+(CPG./(RHO1E.*LEN.*CP1)).*(NW(1:n,1).*(A*T(1:n,1)))-
((DHV.*RHO1)./(RHO1E.*CP1)).*(-KD.*T(2*n+1:3*n,1));
% "Material Balance Equation for Water Vapor (Equation 3.94)"
resid(n+1:2*n,1)=Tdot(n+1:2*n,1)-
((KBULKW+KSELF.*T(n+1:2*n,1)).*(B*T(n+1:2*n,1))
+KSELF.*(A*T(n+1:2*n,1)).*(A*T(n+1:2*n,1)))/(LEN*LEN.*EF)
+(((RHO1.*T(1:n,1).*R)./(EF.*WMWT)).*((-KD.*T(2*n+1:3*n,1))));
```

Table B1.3: Continued.

```
% "The Desorption Rate of Bound Water in the Dried Layer (Equation 3.96)"
resid(2*n+1:3*n,1)=Tdot(2*n+1:3*n,1)+(KD.*T(2*n+1:3*n,1));
% "Boundary Conditions"
resid(1)=-(K1E(1)./LEN).*A(1,:)*T(1:n,1)-(SIG*FAK*(TUP.^4-TYUZ.^4)); % (Equations 3.87 and 3.88)
resid(n)=(K1E(n)./LEN).*A(n,:)*T(1:n,1)-KF*(TAP-T(n,1));  % (Equations 3.89 and 3.91)
resid(n+1)=PWO-T(n+1,1);   % (Equation 3.100)
resid(2*n)=A(n,:)*T(n+1:2*n,1); % (Equation 3.101)
```